

UNCLASSIFIED

AD NUMBER
AD266898
NEW LIMITATION CHANGE
TO Approved for public release, distribution unlimited
FROM Distribution authorized to U.S. Gov't. agencies and their contractors; Administrative/Operational Use; Jul 1961. Other requests shall be referred to Army Signal Research and Development Lab., Fort Monmouth, New Jersey.
AUTHORITY
USAEC ltr, 13 Jan 1970

THIS PAGE IS UNCLASSIFIED

UNCLASSIFIED

AD 266 898

*Reproduced
by the*

ARMED SERVICES TECHNICAL INFORMATION AGENCY
ARLINGTON HALL STATION
ARLINGTON 12, VIRGINIA

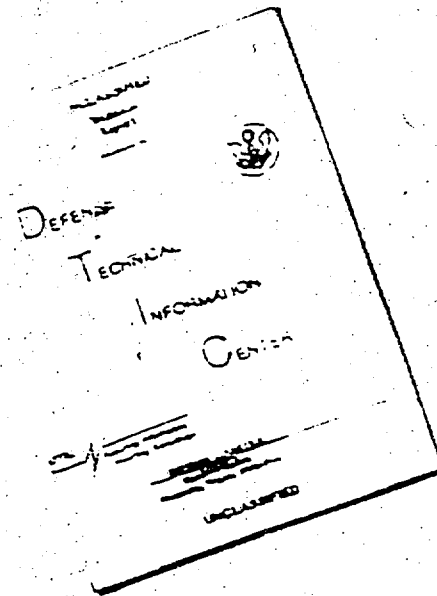


Best Available Copy

NOTICE: When government or other drawings, specifications or other data are used for any purpose other than in connection with a definitely related government procurement operation, the U. S. Government thereby incurs no responsibility, nor any obligation whatsoever; and the fact that the Government may have formulated, furnished, or in any way supplied the said drawings, specifications, or other data is not to be regarded by implication or otherwise as in any manner licensing the holder or any other person or corporation, or conveying any rights or permission to manufacture, use or sell any patented invention that may in any way be related thereto.

Best Available Copy

DISCLAIMER NOTICE



THIS DOCUMENT IS BEST
QUALITY AVAILABLE. THE COPY
FURNISHED TO DTIC CONTAINED
A SIGNIFICANT NUMBER OF
PAGES WHICH DO NOT
REPRODUCE LEGIBLY.

REPRODUCED FROM
BEST AVAILABLE COPY

AS AD NO. 266898
266898

Technical Report No. 151

Case No. 13-145

HEXAGONAL MAGNETIC MATERIALS FOR MICROWAVE APPLICATIONS

Report No. 6

FINAL REPORT

Summary of Work Performed under Contracts
DA-36-039 SC-72319, DA-36-039 SC-73223, DA-36-039 SC-78071
as well as Contract DA-36-039 SC-85279

May 1956 - July 1961

By D. J. De Bitetto, F. K. du Pré and F. G. Brockman

and

SIXTH QUARTERLY PROGRESS REPORT

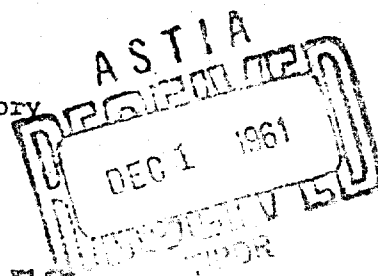
15 April 1961 - 14 July 1961

By D. J. De Bitetto, F. K. du Pré, F. G. Brockman
W. G. Steneck, Jr. and D. W. Krautkopf

Contract No. DA 36-039 SC-85279
DA Project No. 3-93-00-700

U. S. Army
Signal Research and Development Laboratory
Fort Monmouth, New Jersey

PHILIPS LABORATORIES
WASHINGTON-ORANGE, NEW YORK



Best Available Copy

PHILIPS LABORATORIES
A Division of North American Philips Company, Inc.
Irvington on Hudson, New York

Technical Report No. 151

Case No. 13-145

HEXAGONAL MAGNETIC MATERIALS FOR MICROWAVE APPLICATIONS

Report No. 6

FINAL REPORT

Summary of Work Performed under Contracts
DA-36-039 SC-72319, DA-36-039 SC-73223, DA-36-039 SC-78071
as well as Contract DA 36-039 SC-85279

May 1956 - July 1961

By D. J. De Bitetto, F. K. du Pré and F. G. Brockman

and

SIXTH QUARTERLY PROGRESS REPORT

15 April 1961 - 14 July 1961

By D. J. De Bitetto, F. K. du Pré, F. G. Brockman
W. G. Steneck, Jr. and D. W. Krautkopf

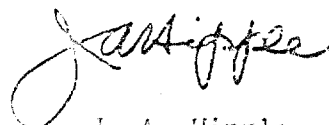
Contract No. DA 36-039 SC-85279
SC Technical Requirements No. SCL-7520, 11 June 1959
DA Project No. 3-93-00-700

U. S. Army
Signal Research and Development Laboratory
Fort Monmouth, New Jersey

OBJECT

Research and development work on materials of the compositional types $\text{BaO} \cdot x[(\text{TiCo})\text{C}_3] \cdot (6-x)\text{Fe}_2\text{O}_3$ and $\text{SrO} \cdot x\text{Al}_2\text{O}_3 \cdot (6-x)\text{Fe}_2\text{O}_3$, aimed at the control of the anisotropy field and the optimization of the microwave properties.

Best Available Copy



J. A. Hipple
Director of Research

HEXAGONAL MAGNETIC MATERIALS FOR MICROWAVE APPLICATIONS

TABLE OF CONTENTS

Final Report

	<u>Page No.</u>
Title Page	i
Table of Contents	ii
List of Figures	iv
Purpose	1
Abstract	3
Publications, Lectures, Reports and Conferences	6
Procedure, Data and Results	7
Introduction	7
I. Summary of the Contracts	9
II. The Materials	10
(a) Crystal Structure of $\text{BaFe}_{12}\text{O}_{19}$ and the Compositions of the Related Materials Studied	10
(b) Preparation of the Materials	16
1. Raw Materials	16
2. Stoichiometry	17
3. Preparation of Anisotropic Samples	18
III. X-Ray Densities of the Compositions	23
IV. Magnetic Properties of the Materials	25
(a) Anisotropy	25
(b) Saturation	27
(c) The Ratio $2K/M$	28
(d) The Coercive Force	29
(e) The Internal Field	30
(f) The Curie Point	31
V. Microwave Magnetic Properties	32
Introduction	32
Experimental Procedure and Results	33
Interpretation of the Results Based on a Simple Model	39
A. $\text{SrO} \cdot x\text{Al}_2\text{O}_3 \cdot (6-x)\text{Fe}_2\text{O}_3$ Series	39
B. $\text{BaO} \cdot x[(\text{TiCo})\text{O}_3] \cdot (6-x)\text{Fe}_2\text{O}_3$ Series	44
VI. Some Remarks on Single Crystal Measurements	47
VII. Examples of the Application of the Aluminum Substituted Materials in Simple Resonance Isolators	48
Engineering Samples Supplied under Contract No. DA 36-039 SC-85279	53
Overall Conclusions	55

(Contd.)

TABLE OF CONTENTS

Sixth Quarterly Progress Report

	<u>Page No.</u>
Abstract	56
Procedure, Data and Results	57
Preparation and Properties of Oriented Magnetic Materials	57
1. Strontium Aluminum Ferric Oxide, $\text{SrO} \cdot 1.7\text{Al}_2\text{O}_3 \cdot 4.3\text{Fe}_2\text{O}_3$	57
2. Barium Titanium Cobalt Ferric Oxide, $\text{BaO} \cdot 0.68[(\text{TiCo})\text{O}_3] \cdot 5.32\text{Fe}_2\text{O}_3$	57
3. Barium Titanium Cobalt Ferric Oxide, $\text{BaO} \cdot 0.78[(\text{TiCo})\text{O}_3] \cdot 5.22\text{Fe}_2\text{O}_3$	57
4. Curie Temperature of $\text{BaO} \cdot 0.78[(\text{TiCo})\text{O}_3] \cdot 5.22\text{Fe}_2\text{O}_3$	63
5. Saturation Magnetization	63
6. Circumferentially Oriented Toroids of $\text{BaO} \cdot 0.48[(\text{TiCo})\text{O}_3] \cdot 5.52\text{Fe}_2\text{O}_3$	63
(a) General Discussion and Fabrication	63
(b) Demonstration of the Oriented Character of the Toroids	68
Microwave Properties	70
Ferrimagnetic Resonance in $\text{BaO} \cdot 0.78[(\text{TiCo})\text{O}_3] \cdot 5.22\text{Fe}_2\text{O}_3$	70

Distribution List	74
-------------------	----

LIST OF FIGURES

Final Report

	Follows Page No.
Fig. 1. Model of the crystal unit cell of $\text{BaO} \cdot 6\text{Fe}_2\text{O}_3$.	10
Fig. 2. Processing procedures for anisotropic materials.	19
Fig. 3. X-ray densities of $\text{BaO} \cdot x\text{Al}_2\text{O}_3 \cdot (6-x)\text{Fe}_2\text{O}_3$ and $\text{SrO} \cdot x\text{Al}_2\text{O}_3 \cdot (6-x)\text{Fe}_2\text{O}_3$.	23
Fig. 4. Saturation per gram, σ , experimental values (room temperature).	28
Fig. 5. Curie temperatures, experimental values.	31
Fig. 6. Block diagram of microwave measurements circuit.	33
Fig. 7. A typical resonance line for Ferroxdure at 57 kmc/sec.	35
Fig. 8. Saturation magnetization as a function of composition for the series $\text{SrO} \cdot x\text{Al}_2\text{O}_3 \cdot (6-x)\text{Fe}_2\text{O}_3$ at 20°C.	39
Fig. 9. Variation of the anisotropy field with composition in $\text{SrO} \cdot x\text{Al}_2\text{O}_3 \cdot (6-x)\text{Fe}_2\text{O}_3$.	41
Fig. 10. Variation of the anisotropy constant with composition in $\text{SrO} \cdot x\text{Al}_2\text{O}_3 \cdot (6-x)\text{Fe}_2\text{O}_3$.	42
Fig. 11. Curie temperature vs x for the series $\text{SrO} \cdot x\text{Al}_2\text{O}_3 \cdot (6-x)\text{Fe}_2\text{O}_3$.	42
Fig. 12. Saturation magnetization as a function of compo- sition for the series $\text{BaO} \cdot x[(\text{TiCo})\text{O}_3] \cdot (6-x)\text{Fe}_2\text{O}_3$ at 20°C.	44
Fig. 13. Variation of the anisotropy field with compo- sition in the series $\text{BaO} \cdot x[(\text{TiCo})\text{O}_3] \cdot (6-x)\text{Fe}_2\text{O}_3$.	45
Fig. 14. Variation of the anisotropy constant with compo- sition in the series $\text{BaO} \cdot x[(\text{TiCo})\text{O}_3] \cdot (6-x)\text{Fe}_2\text{O}_3$.	46
Fig. 15. Curie temperature vs composition for the series $\text{BaO} \cdot x[(\text{TiCo})\text{O}_3] \cdot (6-x)\text{Fe}_2\text{O}_3$.	46

(Contd.)

LIST OF FIGURES

Final Report

	<u>Follows</u> <u>Page No.</u>
Fig. 16. Reverse and forward loss measurements of an E-plane isolator using $\text{SrO} \cdot 0.5\text{Al}_2\text{O}_3 \cdot 5.5\text{Fe}_2\text{O}_3$ with no external field.	42
Fig. 17. Waveguide device for forward and reverse absorption measurements.	49
Fig. 18. Reverse and forward losses of an H-plane slab of $\text{SrO} \cdot 0.2\text{Al}_2\text{O}_3 \cdot 5.8\text{Fe}_2\text{O}_3$ with $H_{ap} = 4100$.	50
Fig. 19. Reverse and forward losses of an H-plane slab of $\text{SrO} \cdot 0.5\text{Al}_2\text{O}_3 \cdot 5.5\text{Fe}_2\text{O}_3$ with $H_{ap} = 0$.	51
Fig. 20. Reverse and forward losses of two H-plane slabs of slightly different composition, arranged in tandem. $H_{ap} = 5800$.	51

Sixth Quarterly Progress Report

Fig. Q-1. Typical resonance absorption line of an E-plane slab (0.003" x 0.100" x 0.80") of $\text{BaO} \cdot 0.78[(\text{TiCo})\text{O}_3] \cdot 5.22\text{Fe}_2\text{O}_3$ at 31.0 kmc/s.	72
---	----

HEXAGONAL MAGNETIC MATERIALS FOR MICROWAVE APPLICATIONS

FINAL REPORT

PURPOSE

1. General

Research and development work on materials of the compositional types $\text{BaO} \cdot x[(\text{TiCo})\text{O}_3] \cdot (6-x)\text{Fe}_2\text{O}_3$ and $\text{SrO} \cdot x\text{Al}_2\text{O}_3 \cdot (6-x)\text{Fe}_2\text{O}_3$, aimed toward the control of the anisotropy field and the optimization of the microwave properties. For this purpose the effects of parameters, such as composition, particle size, orientation, firing temperature and any other variables which are deemed appropriate, shall be investigated.

2. Detail Requirements

The detail requirements of the work under the present contract, DA 36-039 SC-85279, and also of the related work under Contracts DA-36-039 SC-72319, DA-36-039 SC-73223, and DA-36-039 SC-78071, can be summarized as follows:

Prepare and investigate the properties of oriented polycrystalline samples in the series $\text{BaO} \cdot x[(\text{TiCo})\text{O}_3] \cdot (6-x)\text{Fe}_2\text{O}_3$ where x takes the following values: 0; 0.25; 0.48; 0.68; 0.78. These values were chosen with the aim of varying the anisotropy field in these materials from 17,500 to 7000 oersteds, making them potentially useful in the 25-50 kmc/sec range.

Prepare and investigate the properties of oriented polycrystalline samples in the series $\text{SrO} \cdot x\text{Al}_2\text{O}_3 \cdot (6-x)\text{Fe}_2\text{O}_3$ where x takes the following values: 0; 0.1; 0.2; 0.5; 1.0; 1.35; 1.42; 1.50; 1.70. These values were chosen with the aim of varying the anisotropy field in these materials from 19,500 to 50,000 oersteds, making them potentially useful in the 50-150 kmc/sec range.

The permanent magnet properties of the materials (maximum energy product, retentivity, coercive force), when measured at room temperature, shall be as high as is consistent with good microwave characteristics. The materials shall have sufficient mechanical strength to withstand the rigors of military use.

ABSTRACT

This Final Report summarizes not only the work done under this contract but also related work carried out under other contracts beginning in May 1956.

Appended as a separate section is a detailed report of the work performed in the Sixth Quarterly period of this contract.

Anisotropic samples of oxidic magnetic substances possessing hexagonal structures were prepared and studied, both for their permanent magnet properties and for their microwave properties. The compositions of these hexagonal materials were $M^{2+}O \cdot xAl_2O_3 \cdot (6-x)Fe_2O_3$ or $M^{2+}O \cdot x[(TiCo)O_3] \cdot (6-x)Fe_2O_3$ where M^{2+} is either Ba^{2+} or Sr^{2+} as indicated in the text. These materials are therefore derivatives of the material referred to as "Ferroxdure", $BaO \cdot 6Fe_2O_3$.

One special task was performed. This consisted in the production of circumferentially oriented toroids of one of these materials. Details of this work are reported in the attached Sixth Quarterly Report.

An investigation was made of the effect on the microwave properties of the partial replacement of Fe^{3+} by either Al^{3+} or by $(Ti^{4+} + Co^{2+})$ in highly anisotropic permanent magnetic materials of the type $M^{2+}O \cdot 6Fe_2O_3$.

The most striking effect found was due to the rapid change of the room temperature anisotropy field with composition.

In the series $\text{SrO} \cdot x\text{Al}_2\text{O}_3 \cdot (6-x)\text{Fe}_2\text{O}_3$ the anisotropy field was found to increase from 19,300 to 53,400 oersteds by varying x from 0 to 1.7. It is believed that 53,400 oersteds is the largest anisotropy field observed in ferrimagnetic materials. This material exhibits natural ferrimagnetic resonance at about 2 mm wavelengths.

In the series $\text{BaO} \cdot x[(\text{TiCo})\text{O}_3] \cdot (6-x)\text{Fe}_2\text{O}_3$ the anisotropy field was found to decrease from 17,500 to 6500 oersteds by varying x from 0 to 0.78.

In both series the saturation magnetization was found to decrease with increasing x . Also a moderate decrease of the Curie temperature was observed.

The ferrimagnetic resonance linewidth of these materials in the oriented polycrystalline form was found to be about 2000 oersteds; the minimum linewidth observed in some single crystals of these materials is about 50 oersteds. The room temperature g -value of the oriented polycrystalline materials was consistently found to be $g = 1.91$.

A theory was presented to describe the decrease of the saturation magnetization with x . The same theory leads to a description of the decrease of the Curie temperature with composition. This theory is based on an hypothesis concerning the substitution of Fe^{3+} ions in preferential crystallographic sites. An expression for the anisotropy field as a function of x is derived by further assuming that the anisotropy constant per cell is

proportional to the number of (Bohr) moments per cell.

A few simple isolators were made to investigate the usefulness of the aluminum-substituted materials in resonance isolators. It was found that they not only performed satisfactorily, but that those for which $x \geq 0.5$ required no applied field to keep them magnetized, regardless of their shape. The highest value obtained for the ratio of the reverse to forward absorption (in db) was 36. A novel method of broadbanding these isolators, feasible with these special materials, was demonstrated.

Although no isolators were made with the Ti + Co substituted materials, the insertion losses of several members of this series as well as several of the Al series were investigated. The resulting low losses obtained indicated that these materials should be useful for resonator applications. It can be concluded that with the above two series of compounds, it is possible to tailor-make microwave magnetic materials having anisotropy fields in the range 7000 to over 50,000 oersteds; these, then, would be useful in the frequency range 25-150 kmc/sec.

PUBLICATIONS, LECTURES, REPORTS AND CONFERENCES

A paper entitled "Magnetic Materials for Use at High Microwave Frequencies (50-90 kMc/sec)", by F. K. du Pré, D. J. De Bitetto, and F. G. Brockman was published (J. Appl. Phys. 29, No. 7, 1127 (1958)).

A paper entitled "Highly Anisotropic Magnetic Materials for Millimeter Wave Applications", by D. J. De Bitetto, F. K. du Pré, and F. G. Brockman was presented at the Ninth International Symposium on Millimeter Waves on 31 March 1959 in New York City. This paper was also published in The Proceedings of the Symposium on Millimeter Waves, Volume IX, by Polytechnic Press, N. Y., 1959.

A paper entitled "Ferrimagnetic Linewidth of Single Crystals of Barium Ferrite ($\text{BaFe}_{12}\text{O}_{19}$)" was jointly published by I. Bady and T. Collins (of the USASRDL), and D. J. De Bitetto and F. K. du Pré (Proc. IRE 48, No. 12, 2033 (1960)).

PROCEDURE, DATA AND RESULTS

Introduction

In the work of the contracts summarized in this report, substitutional compounds of the types $M^{2+}O \cdot x(Al_2O_3) \cdot (6-x)Fe_2O_3$ and $M^{2+}O \cdot x[(TiCo)O_3] \cdot (6-x)Fe_2O_3$ were investigated. It was shown that the microwave natural resonant frequency varies approximately as the ratio of the anisotropy constant K divided by the saturation magnetization M . Twice this ratio is equal to the internal or crystalline anisotropy field, i.e., $H_{an} = \frac{2K}{M}$. By replacement of the Fe^{3+} ions by Al^{3+} in the first of the above-mentioned series, both M and K were found to decrease, M decreasing faster than K . This resulted in an increase in the anisotropy field to values greater than 50,000 oersteds (and a corresponding increase in the microwave natural resonant frequency) with increasing Al content. In this work M^{2+} was taken to be either Ba or Sr , the results being very similar in both cases. A theoretical expression was developed for the variation of the anisotropy field with composition. Microwave measurements of H_{an} allowed a check on the validity of the theory. The theory, although good for small x , gradually worsens for larger x .

A different approach must be taken in order to decrease the anisotropy field below that of $M^{2+}O \cdot 6Fe_2O_3$. For the compound $BaO \cdot 6Fe_2O_3$ it was found possible to accomplish this by simultaneously substituting one Ti^{4+} and one Co^{2+} for two Fe^{3+} ions.

It was assumed that this would also be the case for $\text{SrO} \cdot 6\text{Fe}_2\text{O}_3$; however, this assumption was found to be invalid. Therefore only the Ba series was investigated in detail. Again both K and M decrease with increasing values of x, but in this series, K decreases faster than M. This resulted in a decrease with x of the anisotropy field (to values lower than 7000 oersteds).

A theoretical expression was developed for the variation of the anisotropy field with composition; this expression is in good agreement with the experimental results.

I. Summary of the Contracts

This Final Report under Contract DA-36-039 SC-85279 also carries a summary of related work* carried out under Contracts DA-36-039 SC-72319, DA-36-039 SC-73223, and DA-36-039 SC-78071.

For convenience in making reference to the various reports under the various contracts, we have numbered the reports serially, beginning with 1 as the first quarterly report of Contract No. DA-36-039 SC-42503.* Accordingly, the cross references used here will be those in Table I.

TABLE I

Contracts Summarized in this Final Report
with Serial Numbers of Reports

<u>Contract No.</u>	<u>Quarterly Reports</u>	<u>Final Report</u>
DA-36-039 SC-72319	13, 14, 15	16
" SC-73223	17, 18, 19	20
" SC-78071	21, 22, 23	24
" SC-85279	25, 26, 27, 28, 29	30

* Work was carried out under Contract No. DA-36-039 SC-42503 (1952-1954) and also under Contract No. DA-36-039 SC-56759 (1954-1955); this work is not specifically summarized here. These two contracts dealt with investigations of the permanent magnet material which serves as the basis of the later work. The investigations were concerned with, first, the techniques for producing the optimum permanent magnet properties of isotropic ceramic magnets and, second, the techniques for producing the optimum permanent magnet properties of oriented ceramic magnets.

Only the work involving the microwave properties of these materials is included in this summary.

II. The Materials

The materials made and investigated in these studies are all related to $\text{BaFe}_{12}\text{O}_{19}$. This material has been developed¹⁾ as a permanent magnet material and is known under various trade names, for instance, Ferroxdure or Magnadur.

(a) Crystal Structure of $\text{BaFe}_{12}\text{O}_{19}$ and the Compositions of the Related Materials Studied

The crystal structure of $\text{BaFe}_{12}\text{O}_{19}$ is the same as that of the mineral magnetoplumbite.²⁾ Figure 1 is a photograph of a crystal model of the unit cell of the structure. In the model, the larger white spheres represent oxygen ions, the large dark ones barium, and the smaller spheres represent ferric iron ions.

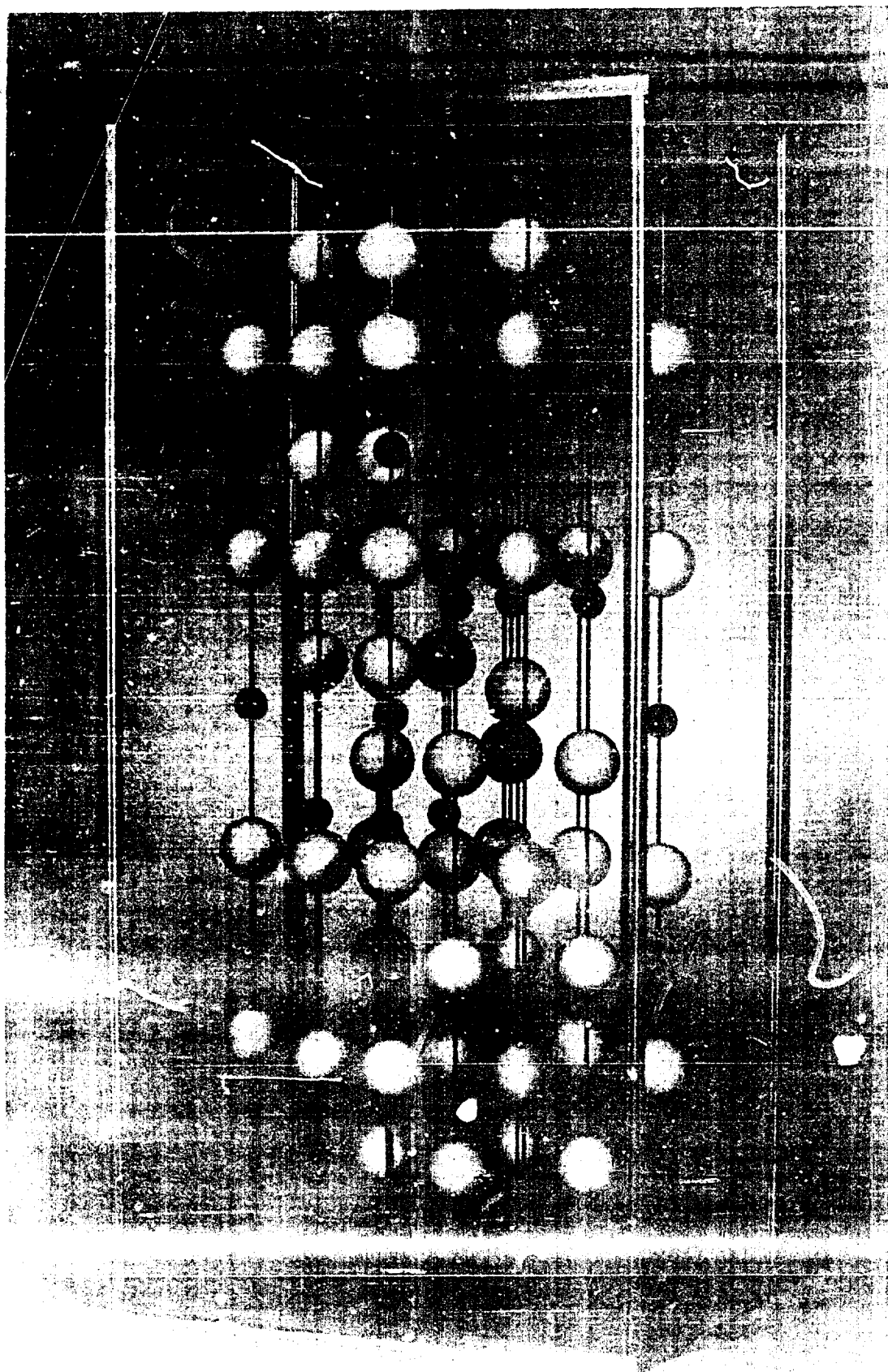
The unit cell dimensions are: $c = 23$ angstroms and $a = 5.9$ angstroms. That is, the unit cell is much longer in the direction of the hexagonal axis than it is in the principal crystallographic direction in the basal plane, perpendicular to the hexagonal axis.

This type of structure can be maintained if the divalent barium ion is replaced by other divalent ions, providing that the ionic radius of the divalent replacement does not differ greatly

1) Went, et al., Philips Tech. Rev. 13, 194-208 (1952).

2) V. Adelskold, Arkiv fuer Kemi, Mineralog. och Geologi, 12A, 1-9 (1938).

Fig. I MODEL OF THE CRYSTAL UNIT CELL OF
 $\text{BaO} \cdot 6\text{Fe}_2\text{O}_3$



Best Available Copy

from the barium ionic radius. Table II gives the ionic radii of ions of interest.³⁾

TABLE II

Ionic Radii, in Angstroms

Ba ²⁺ 1.43	Fe ³⁺ 0.67
Pb ²⁺ 1.32	Al ³⁺ 0.57
Sr ²⁺ 1.27	Co ²⁺ 0.82
Ca ²⁺ 1.06	Ti ⁴⁺ 0.64
	Co ³⁺ 0.64
	Ti ³⁺ 0.69

From Table II it can be imagined that the barium ion can be replaced by lead and by strontium and this is the case as previously shown.²⁾ The ionic radius of calcium ion is too small to form a stable "magnetoplumbite" structure, but a fraction of the barium can be replaced by calcium without destroying the symmetry.⁴⁾

Adelskold²⁾ has shown also that the compounds $\text{CaAl}_{12}\text{O}_{19}$, $\text{SrAl}_{12}\text{O}_{19}$ and $\text{BaAl}_{12}\text{O}_{19}$ likewise have the "magnetoplumbite" structure.

It is therefore possible to prepare ferrimagnetic materials which possess the magnetoplumbite structure in which the barium may be completely replaced by lead and strontium and partially by calcium.

3) Taschenbuch fuer Chemiker, u. Physiker, D'Ans & Lax, Springer, Berlin (1949).

4) J. J. Went, et al., U. S. patent 2,762,777.

In addition, the iron may be partially* replaced by aluminum. In discussing these substituted compounds it is convenient to rewrite the formula of $\text{BaFe}_{12}\text{O}_{19}$ as $\text{BaO} \cdot 6\text{Fe}_2\text{O}_3$. Then a more general formula may be written to indicate the various substitutions which will be considered here. This general formula is: $\text{M}^{2+}\text{O} \cdot x(\text{N}^{3+}_2\text{O}_3) \cdot (6-x)\text{Fe}_2\text{O}_3$. In this formula M^{2+} represents Ba^{2+} , Sr^{2+} or Pb^{2+} and (partially) Ca^{2+} ; N^{3+} represents in this work Al^{3+} (although other trivalent ions have been introduced by other workers).

There are a number of literature references which deal with aluminum substitutions in the magnetoplumbite structure and the effect of these substitutions upon the magnetic properties of the materials.⁵⁻⁹ (Some of these references report also the substitution of trivalent ions other than Al^{3+} .) Eleven compositions from $x = 0$ to $x = 1.70$ have been prepared under various contracts. Table III, which follows the next discussion, contains a listing of all compositions made.

* Indeed, according to ²⁾, complete replacement can yield the compounds $\text{CaAl}_{12}\text{O}_{19}$, $\text{SrAl}_{12}\text{O}_{19}$ and $\text{BaAl}_{12}\text{O}_{19}$, but, obviously, these are of no interest here since no ferrimagnetic behavior will exist upon the complete exclusion of the ferric ion.

- 5) H. Kojima, Sci. Rep. Research Inst., Tohoku Univ. A7, 507-514 (1955).
- 6) Guillaud & Villers, Compt. rend. 242, 2817-2820 (1956).
- 7) Van Uitert, J. Appl. Phys. 28, 317-319 (1957).
- 8) Mones & Banks, J. Phys. Chem. Solids, 4, 217-222 (1958).
- 9) Bertaut, Deschamps & Pauthenet, Compt. rend. 246, 2594-97 (1958).

As discussed above, certain trivalent ions (here Al^{3+}) may be substituted for Fe^{3+} ion in the magnetoplumbite lattice. However, there is another sort of substitution which can be made without the loss of the structure. This type of substitution depends upon the replacement of Fe^{3+} ion by equimolar amounts of a divalent ion and a quadrivalent ion. The requirement is that the ionic radii of these ions do not greatly differ from that of the Fe^{3+} ion. In this case, two gram ions of Fe^{3+} are replaced by one gram ion of the divalent ion and one gram ion of the quadrivalent ion.

Compositions in which such divalent-quadrivalent substitutions have been made are described in the literature.¹⁰⁾ Of the various possible ionic substitutions of this sort, one is of special interest. (The reason for this special interest will appear in the discussion of the magnetic properties of the materials.) This special substitution¹¹⁾ is the equimolar substitution of Co^{2+} and Ti^{4+} for 2Fe^{3+} . Reference to Table II will show that the ionic radii* of the three ions are similar and

10) Smit and Wijn, "Ferrites", Philips Technical Library, Eindhoven (1959).

11) E. W. Gorter, U. S. Patent 2,960,471.

* Cobalt and titanium both enter into chemical combination in the trivalent state. It is interesting to note that the ionic radii of Fe^{3+} , Co^{3+} and Ti^{3+} are, respectively, 0.67, 0.64 and 0.69. This strongly suggests that, in these materials, the cobalt and titanium exist in the trivalent state. In the trivalent state titanium has one uncompensated 3d electron and therefore one Bohr magneton, whereas in the quadrivalent state there are no uncompensated electrons. Similarly, the number of Bohr magnetons for cobalt ion increases by one in going from the divalent to the trivalent state.

substitution does therefore occur. It might be imagined that Ba^{2+} may be replaced by Co^{2+} but reference to the Table , shows the large difference in these ionic radii which prevents this substitution. Table III which follows lists all compositions made and studied under the contracts mentioned.

Some explanation concerning the inclusion of both barium containing and strontium containing compositions is in order here.

In the first microwave studies carried out in these contracts, $\text{BaO} \cdot 6\text{Fe}_2\text{O}_3$ and $\text{SrO} \cdot 6\text{Fe}_2\text{O}_3$ were compared. The strontium based material, $\text{SrO} \cdot 6\text{Fe}_2\text{O}_3$, insofar as its microwave losses were concerned, was comparable to the barium based material in the X band of frequencies, but in the K band it was superior to the barium material.

As a result the strontium base was used for the substitution experiments and all but one of the aluminum substituted compositions were made on this basis. (The one barium-aluminum composition was in process while the above K-band data were being accumulated.)

The cobalt-titanium substitution compositions were begun also in the strontium system. However, it became apparent in the microwave studies that the anticipated* internal fields (q.v.) of

* Our anticipations were based on a private communication from Ir. H. G. Beljers, Philips Research Laboratories, Eindhoven, Netherlands. He reported an internal field of 7000 oersteds for $\text{BaO} \cdot 0.66[(\text{TiCo})\text{O}_3] \cdot 5.34\text{Fe}_2\text{O}_3$. These data and our own value of the internal field of $\text{BaO} \cdot 6\text{Fe}_2\text{O}_3$ were used to predict three compositions with internal fields of 10,000, 13,000 and 16,000 oersteds. It was not expected that the substitution of strontium for barium would have the pronounced effect that it did have.

TABLE III

Compositions Prepared and Studied together
with Cross References to Earlier Reports

<u>Composition</u>	<u>Report Serial No. as per Table I</u>
<u>Barium Containing</u>	
$\text{BaO} \cdot 6 \text{Fe}_2\text{O}_3$	13, 14, 15
$\text{BaO} \cdot 1.0 \text{Al}_2\text{O}_3 \cdot 5.0 \text{Fe}_2\text{O}_3$	17
$\text{BaO} \cdot 0.25 [(\text{TiCo})\text{O}_3] \cdot 5.75 \text{Fe}_2\text{O}_3$	25, 26, 27
$\text{BaO} \cdot 0.48 [(\text{TiCo})\text{O}_3] \cdot 5.52 \text{Fe}_2\text{O}_3$	23, 24, 28
$\text{BaO} \cdot 0.68 [(\text{TiCo})\text{O}_3] \cdot 5.32 \text{Fe}_2\text{O}_3$	25, 26, 27, 28
$\text{BaO} \cdot 0.78 [(\text{TiCo})\text{O}_3] \cdot 5.22 \text{Fe}_2\text{O}_3$	29
<u>Strontium Containing</u>	
$\text{SrO} \cdot 6 \text{Fe}_2\text{O}_3$	13, 14, 15, 16, 20
$\text{SrO} \cdot 0.1 \text{Al}_2\text{O}_3 \cdot 5.9 \text{Fe}_2\text{O}_3$	18, 19, 20
$\text{SrO} \cdot 0.2 \text{Al}_2\text{O}_3 \cdot 5.8 \text{Fe}_2\text{O}_3$	18, 19, 20
$\text{SrO} \cdot 0.5 \text{Al}_2\text{O}_3 \cdot 5.5 \text{Fe}_2\text{O}_3$	18, 19, 20
$\text{SrO} \cdot 1.0 \text{Al}_2\text{O}_3 \cdot 5.0 \text{Fe}_2\text{O}_3$	18, 19, 20
$\text{SrO} \cdot 1.35 \text{Al}_2\text{O}_3 \cdot 4.65 \text{Fe}_2\text{O}_3$	21
$\text{SrO} \cdot 1.42 \text{Al}_2\text{O}_3 \cdot 4.58 \text{Fe}_2\text{O}_3$	25
$\text{SrO} \cdot 1.50 \text{Al}_2\text{O}_3 \cdot 4.50 \text{Fe}_2\text{O}_3$	25
$\text{SrO} \cdot 1.70 \text{Al}_2\text{O}_3 \cdot 4.30 \text{Fe}_2\text{O}_3$	27, 28
$\text{SrO} \cdot 0.16 [(\text{TiCo})\text{O}_3] \cdot 5.84 \text{Fe}_2\text{O}_3$	21, 22, 23, 24
$\text{SrO} \cdot 0.32 [(\text{TiCo})\text{O}_3] \cdot 5.68 \text{Fe}_2\text{O}_3$	21, 22, 23, 24
$\text{SrO} \cdot 0.48 [(\text{TiCo})\text{O}_3] \cdot 5.52 \text{Fe}_2\text{O}_3$	21, 22, 23, 24

the compositions chosen were not achieved. One composition in the barium system ($\text{BaO} \cdot 0.48[(\text{TiCo})\text{O}_3] \cdot 5.52\text{Fe}_2\text{O}_3$) was then made and considerably better agreement between expectation and actual experiment resulted. Therefore, all later cobalt-titanium substituted compositions were based on the barium system. The reason that the strontium-cobalt-titanium materials did not possess internal fields closer to the internal fields of similar barium materials was not established.

(b) Preparation of the Materials

1. Raw Materials

All the materials studied were made by sintering techniques.* The starting materials were appropriate compounds of the various cations. These appropriate compounds were either the oxides or carbonates. The following raw materials have been used in one or another of the various final materials prepared:

Barium Carbonate, Precipitated Purified
Strontium Carbonate, Reagent Grade
Ferric Oxide, C. K. Williams, R-1899
Aluminum Oxide, Linde, B-5125, 99.99% pure
Cobaltous Carbonate, Reagent Grade
Titanium Dioxide, " "

Of these raw materials, the Linde aluminum oxide was accepted at the stated purity given by the manufacturer. All other raw materials were subjected to chemical assays and

* A few single crystals were also studied. These were obtained from outside sources and their method of preparation will not be discussed.

appropriate corrections were made in the stoichiometric calculations to account for the departures from 100% purity.

2. Stoichiometry

Throughout this report the compositions of the materials are reported on the basis of one mole of BaO or SrO to 6 moles of Fe_2O_3 (or a total of 6 moles when substitution of Fe_2O_3 is indicated; thus: $\text{BaO} \cdot 0.78[(\text{TiCo})\text{O}_3] \cdot 5.22\text{Fe}_2\text{O}_3$).

This, however, is not the basis on which the compositions were prepared. Raw materials were processed on the basis 1.1 BaO or 1.1 SrO to 6.0 Fe_2O_3 (or the total of 6 moles when substitution of Fe_2O_3 is indicated).

The early phases of this contract work (not specifically summarized here) were concerned with the permanent magnet properties of materials related to $\text{BaO} \cdot 6\text{Fe}_2\text{O}_3$. In this early work it was demonstrated that superior permanent magnet properties were developed if, in the initial raw materials, the ratio of barium to iron was greater than that indicated (i.e. 1:6). The optimum was found to be 1.1:6.0. This ratio has been maintained throughout the subsequent work. In reporting the compositions of the materials prepared, it was our custom to specify this deviation from stoichiometry. For instance, $1.1\text{BaO} \cdot 0.78[(\text{TiCo})\text{O}_3] \cdot 5.22\text{Fe}_2\text{O}_3$ for the example above. However, in the Quarterly Progress Report, 15 January 1960 to 14 April 1960 (Table I, No. 25) the departure from stoichiometry was deleted from the symbolic formulae. The principal reason for this change was that the literature then began

to contain numerous references to these materials, and in these references the compositions are usually stated on the basis of the 1:6 ratio. It is our assumption that the intrinsic properties which are observed are those of the stoichiometric materials. Therefore, in order to avoid confusion in comparing our results with data presented by other workers, we began with Report 25, (Table I) to report our compositions on the 1:6 basis, although the compositions were prepared on the 1.1 to 6.0 basis in the initial raw materials.

We feel a certain justification for our assumption that the intrinsic properties are those of the stoichiometric materials, for we have furnished chemical evidence of a second phase which we identified as BaO (or SrO as the case may be). This second phase was not detectable by X-ray diffraction analysis. We have expressed the opinion that one of the virtues of this second phase is its influence on the structure sensitive properties of the material, especially the coercive force.

If the second phase in the solid samples is BaO (or SrO), the 0.1 mol excess corresponds to a dilution of the magnetic phase by about 1.4% by weight in the case of $\text{BaO} \cdot 6\text{Fe}_2\text{O}_3$ and by about 1.0% in the case of $\text{SrO} \cdot 6\text{Fe}_2\text{O}_3$.

3. Preparation of Anisotropic Samples

Except for a few early experiments on polycrystalline isotropic samples, all work reported here has dealt with anisotropic polycrystalline samples. That the uniaxial hexagonal magnetic material $\text{BaO} \cdot 6\text{Fe}_2\text{O}_3$ can be prepared in highly oriented state has been described previously.¹²⁾

12) Stuijts, Rathenau & Weber, Philips Tech. Review 16, 141-147 (1954).

In the preparation of anisotropic samples, the material is first prepared by solid state reactions so that crystallites, which are definitely larger than single domain size, are grown. This then is ground to prepare a powder in which most of the particles are smaller than single domain size, but still fragments of single crystals. The powder so prepared is then pressed in the presence of a strong magnetic field to form a piece suitable for final firing.

The process is long and involved and is best described by reference to Fig. 2, Processing Procedures for Anisotropic Materials.

In Fig. 2 are shown the 14 steps involved in the preparation of the anisotropic samples. Details concerning these various steps follow.

Step 1. The quantities of raw materials necessary were calculated on the basis of the required stoichiometry. Allowance was made for the assayed percentage purity of each raw material. These then were weighed out in the required amounts.

Step 2. The raw materials were thoroughly mixed in a high speed mixer using ethyl alcohol as the blending agent.

Step 3. The blending fluid was removed from the blended raw materials by simple filtration. The blended materials were then dried at about 120°C.

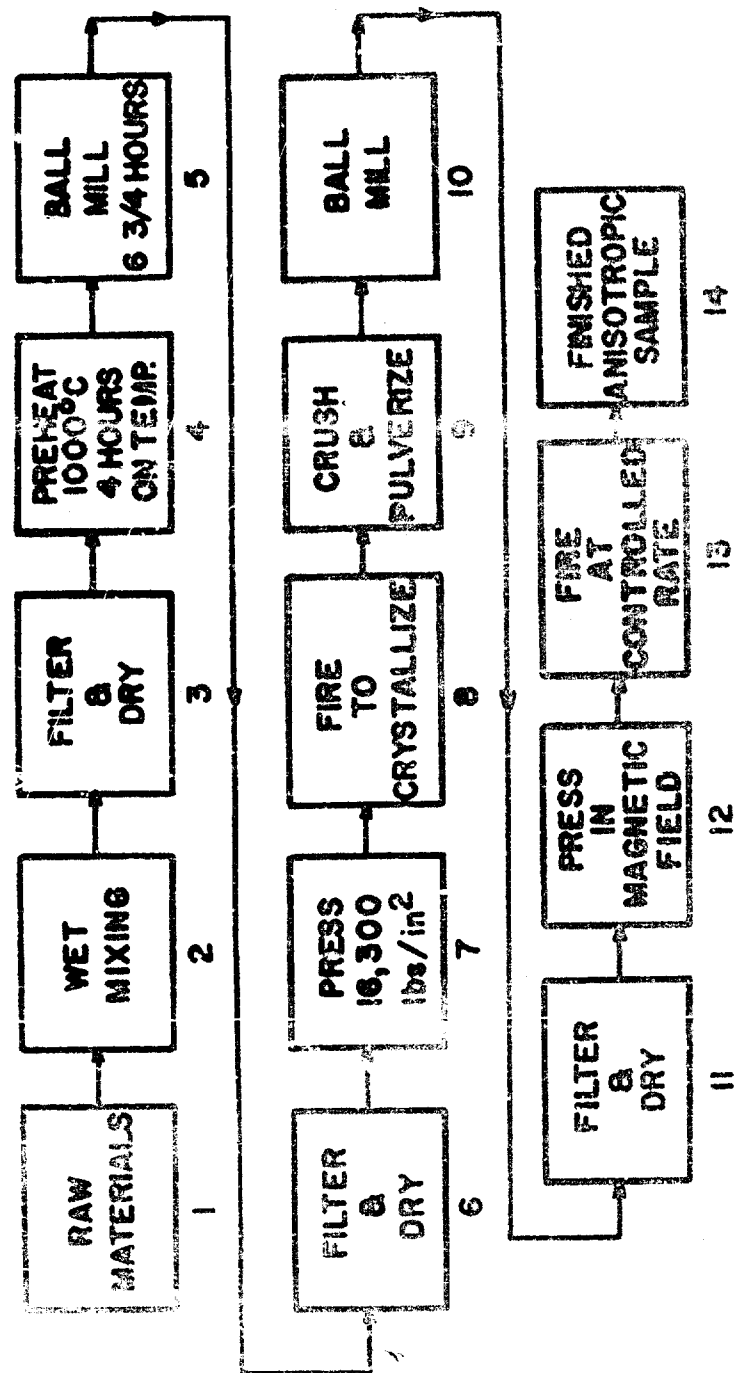


Fig. 2

PROCESSING PROCEDURES FOR
ANISOTROPIC MATERIAL

Step 4. The material from Step 3 was broken up and transferred to Alundum crucibles. Prefiring of this powder for 4 hours at 1000°C then produced a partly reacted material.

Step 5. This ball milling was carried out using ethyl alcohol as the milling agent.

Step 6. The milled powder was separated from the milling agent by simple filtration.

Step 7. This partly reacted powder was pressed into slugs 1" in diameter and about 1-1/2" to 2" tall.

Step 8. The slugs of Step 7 were fired and an effort was made to carry out the firing at a sufficiently high temperature and for a sufficiently long time to produce crystallites on the slugs which are easily visible to the naked eye. These firing conditions depend upon the refractory nature of the material. Usually the firing temperature was between 1300° and 1400°C and the time about 4 hours.

Step 9. The crystallized slugs were crushed in a jaw crusher and then pulverized in a Braun pulverizer.

Step 10. This ball milling was carried out with ethyl alcohol as the milling fluid. The particle size of the resulting powder is of some importance especially as it affects Step 12. In general,

the milling time lay between 10 and 100 hours. For the various preparations, reference should be made to the reports dealing with the particular composition for details concerning this milling operation.

Step 11. The milled powder was separated from the milling agent by simple filtration.

Step 12. All samples were pressed in a 1" x 1" single-acting die.* The usual sample weight was 30 grams and the pressed height was about 1.7 cm.

The die was equipped with holes in the two die faces in the pressing direction. These holes were covered for each pressing with squares of filter paper.

The 30 grams of powder were thoroughly mixed with 40 cc of a 2% polyvinylalcohol solution. This slurry was introduced into the die and the whole unit was placed between the 4" pole pieces of an electromagnet, so that a magnetic field could be established along one of the 1" directions, perpendicular to the pressing direction.

A field of about 7000 oersteds was applied for about 10 seconds and then reduced to about 5500 oersteds.

Pressing of the slurry was then begun. The 5500 oersted

* Except for circumferentially oriented toroids specially made at the request of the USASRDL for experiments to be conducted by Melabs, Palo Alto, Calif. Since making such toroids is a special problem, the techniques are described separately in the Sixth Quarterly Report bound with this report.

field was applied throughout the time for pressing. The pressure was raised slowly so that the water of the slurry could be removed through the filter papers. The final pressure was about 3000 pounds per sq. in.

In some cases, rod shaped samples were required. These were made by cutting them out of a "green" piece pressed in the 1" x 1" die. Usually the axis of the cylindrical rod was taken in the direction of the original orienting field.

Step 13. Firing of the oriented, pressed pieces was carried out in air. The temperature of firing depended on the refractory nature of the material. The usual temperatures were between 1200° and 1400°C. The time on temperature was usually 1 hour. Reference should be made to the reports dealing with particular compositions, see Tables I and III.

In general, the dimensional shrinkage upon firing was anisotropic. The shrinkage in the oriented direction (i.e. the direction of the hexagonal axis, alternatively, the direction of the orienting field) being greater than in the two directions perpendicular to this direction. The fired dimension of a typical sample was 1.86 cm in the oriented direction, 2.24 cm in the direction perpendicular to this direction, and 1.50 cm in the pressed direction (also perpendicular to the oriented direction).

III. X-Ray Densities of the Compositions

As will be discussed below (see section "IV (b) Saturation"), the observed saturation magnetizations may be converted to saturation magnetization per unit volume at X-ray density from the measured apparent density and the X-ray density. The X-ray densities of the aluminum substituted materials were determined in the following manner.

In the absence of other information it may be assumed that the densities of solid solutions of $\text{BaO} \cdot 6\text{Fe}_2\text{O}_3$ and $\text{BaO} \cdot 6\text{Al}_2\text{O}_3$ as well as the densities of solid solutions of $\text{SrO} \cdot 6\text{Fe}_2\text{O}_3$ and $\text{SrO} \cdot 6\text{Al}_2\text{O}_3$ will vary linearly with composition expressed in mole percent. (This is an extension of Vegard's rule with regard to the lattice parameters of substitutional solutions of the elements.)

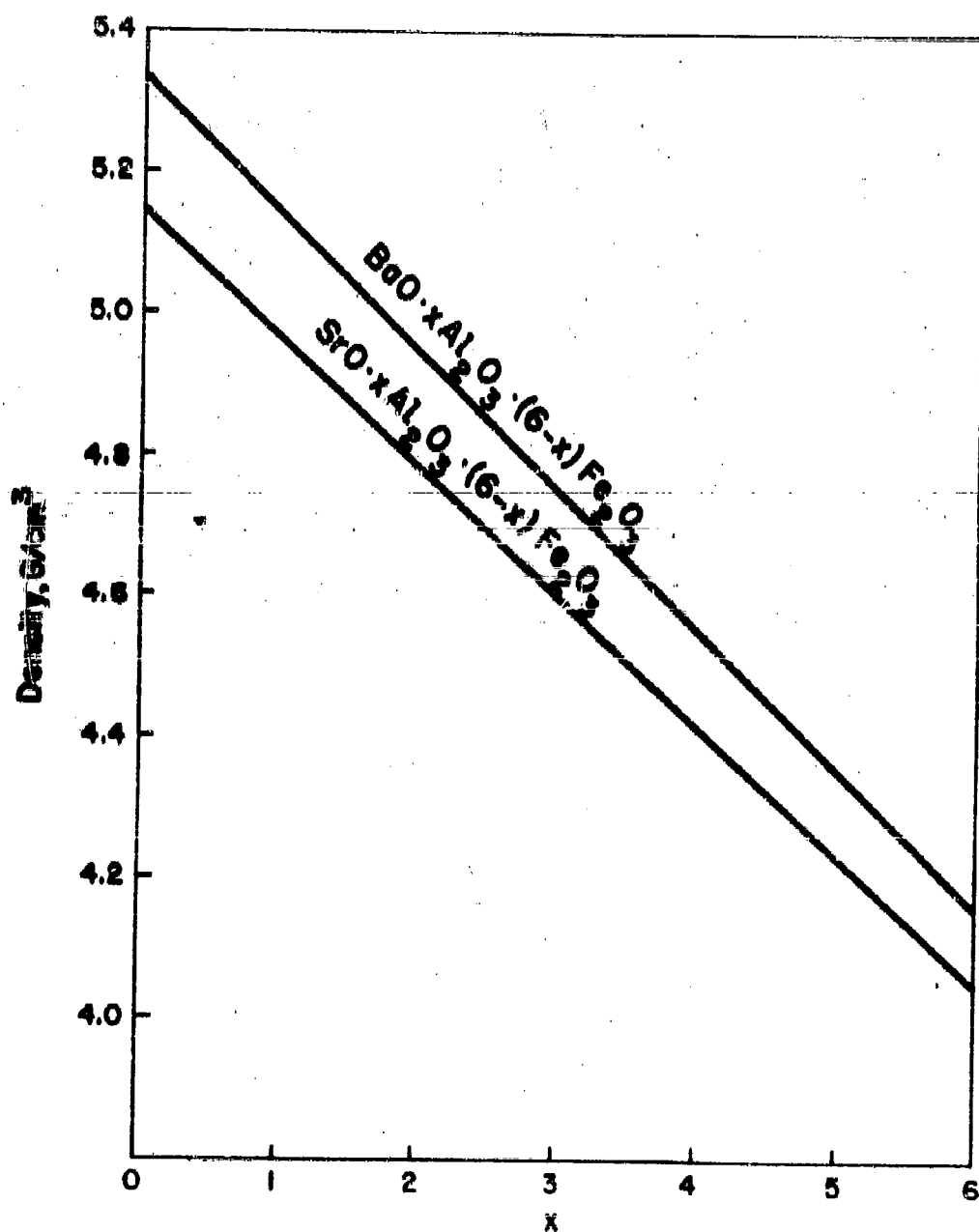
The X-ray densities of the four compounds immediately above were calculated. Adelskold²⁾ has given the lattice parameters of these compounds. Using his data and the mass of an atom of unit atomic weight to be 1.6603×10^{-24} gram, the calculated X-ray densities are:

$\text{BaO} \cdot 6\text{Fe}_2\text{O}_3$	5.33 Gm/cm ³	$\text{SrO} \cdot 6\text{Fe}_2\text{O}_3$	5.14 Gm/cm ³
$\text{BaO} \cdot 6\text{Al}_2\text{O}_3$	4.16 Gm/cm ³	$\text{SrO} \cdot 6\text{Al}_2\text{O}_3$	4.05 Gm/cm ³

On the basis of the above linear assumption and these data, Fig. 3 was drawn. This serves to give the X-ray densities of the various solid solutions.

Similar data are not available for the calculation of the X-ray densities of the series $\text{BaO} \cdot x[(\text{TiCo})\text{O}_3] \cdot (6-x)\text{Fe}_2\text{O}_3$.

Fig.3 X-RAY DENSITIES
 $\text{BaO} \cdot x\text{Al}_2\text{O}_3 \cdot (6-x)\text{Fe}_2\text{O}_3$ & $\text{SrO} \cdot x\text{Al}_2\text{O}_3 \cdot (6-x)\text{Fe}_2\text{O}_3$



Accordingly the cooperation of the X-Ray Section was enlisted and the unit cell dimensions of three compositions were determined. In addition, the unit cell dimensions of $\text{BaO} \cdot 6\text{Fe}_2\text{O}_3$ were determined. The results follow:

	a	c
$\text{BaO} \cdot 6\text{Fe}_2\text{O}_3^*$	5.902	23.23
$\text{BaO} \cdot 0.48[(\text{TiCo})\text{O}_3] \cdot 5.52\text{Fe}_2\text{O}_3$	5.87	23.2
$\text{BaO} \cdot 0.68[(\text{TiCo})\text{O}_3] \cdot 5.32\text{Fe}_2\text{O}_3$	5.88	23.2
$\text{BaO} \cdot 0.78[(\text{TiCo})\text{O}_3] \cdot 5.22\text{Fe}_2\text{O}_3$	5.88	23.2

There is no really significant change in the X-ray densities over the concentration range of $[(\text{TiCo})\text{O}_3]$ substitution used here. Within the precision of the measurements, the solid solutions $\text{BaO} \cdot x[(\text{TiCo})\text{O}_3] \cdot (6-x)\text{Fe}_2\text{O}_3$ all have the same unit cell dimensions. The change in molecular weight in going from $\text{BaO} \cdot 6\text{Fe}_2\text{O}_3$ to $\text{BaO} \cdot 0.78[(\text{TiCo})\text{O}_3] \cdot 5.22\text{Fe}_2\text{O}_3$ is 1111.6 to 1107.8 or about 0.3%. If it is assumed that the difference shown in the lattice parameters is significant, then the X-ray density of $\text{BaO} \cdot 0.78[(\text{TiCo})\text{O}_3] \cdot 5.22\text{Fe}_2\text{O}_3$ is about 2 parts in 1000 greater than that of $\text{BaO} \cdot 6\text{Fe}_2\text{O}_3$. Some doubt may exist concerning the significance of this difference since the X-ray report indicated that, for the substituted materials, the lines were weak, of poor quality and not well resolved.

* The parameters of $\text{BaO} \cdot 6\text{Fe}_2\text{O}_3$ differ slightly from those reported by Adelskold²⁾ and used in the preparation of Fig. 3. His values are: $\text{BaO} \cdot 6\text{Fe}_2\text{O}_3$ $a = 5.876$ $c = 23.17$

On the basis of the above reported X-ray investigation, it may be assumed that the X-ray density of $\text{BaO} \cdot 6\text{Fe}_2\text{O}_3$, i.e. 5.33 gm/cm^3 , applies also to the corresponding titanium-cobalt substitution compounds up to $x = 0.78$ in $\text{BaO} \cdot x[(\text{TiCo})\text{O}_3] \cdot (6-x)\text{Fe}_2\text{O}_3$.

IV. Magnetic Properties of the Materials

(a) Anisotropy

The material $\text{BaFe}_{12}\text{O}_{19}$ has one axis of easy magnetization parallel to the hexagonal axis (i.e. the crystal anisotropy is uniaxial).

The tendency of a magnetic material to possess this uniaxial preferred direction of magnetization may be described by the amount of energy, E , necessary to turn the magnetization from the easy direction through an angle θ . E is given by:

$$E = K_1 \sin^2 \theta + K_2 \sin^4 \theta + \dots$$

where the quantities K_1 , K_2 etc. are constants (which, however, are functions of temperature).

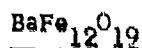
In the case of $\text{BaFe}_{12}\text{O}_{19}$ the first term is sufficient to describe the behavior so that the energy becomes

$$E = K \sin^2 \theta .$$

For $\text{BaFe}_{12}\text{O}_{19}$ the constant K has been reported to be $3 \times 10^6 \text{ erg/cm}^3$.¹⁾ In this work, the value of the constant K for $\text{BaFe}_{12}\text{O}_{19}$ was determined on a well oriented polycrystalline sample by the measurement of the energy difference between the magnetization process in the easy (hexagonal axis) direction and in a

direction at right angles to the hexagonal axis (Report 15, Table I).

The value obtained was:



Room temperature

$$K = 2.8 \times 10^6 \text{ ergs per cm}^3$$

In a similar manner the anisotropy constant for $\text{SrFe}_{12}\text{O}_{19}$ has been determined (Report 16).



Room temperature

$$K = 3.3 \times 10^6 \text{ ergs per cm}^3$$

This technique is not applicable to the determination of the anisotropy constant of the aluminum substituted materials since it becomes impossible to saturate these materials in the "difficult" direction (i.e. at right angles to the oriented direction) with fields which can be generated in our laboratory (certain of these materials require fields in excess of 40,000 oersteds for saturation).

However, microwave resonance techniques, to be discussed later, make possible the determination of this quantity for all compounds studied.

In the titanium-cobalt substituted materials it is known¹⁰⁾ that the anisotropy decreases with increased replacement of Fe^{3+} . Indeed, at the composition $\text{BaO} \cdot 1.2[(\text{TiCo})\text{O}_3] \cdot 4.8\text{Fe}_2\text{O}_3$

the anisotropy constant is zero. This zero is evidence that, for replacements in excess of 1.2, the easy direction of magnetization is no longer the direction of the hexagonal axis, but at right angles to this direction, that is, in the basal plane.¹⁰⁾ Other oxidic magnetic substances possessing this type of anisotropy have been described and have been referred to as Ferroxlana materials.^{13,14)}

This work has been concerned with only those titanium-cobalt substituted compositions possessing uniaxial anisotropy, (i.e. those in which the substitution is less than the 1.2 of the above formula).

There was some indication that one constant in the energy expression given above may not be sufficient to describe the anisotropy in some of the higher substitutions studied here.

(b) Saturation

The saturation magnetizations for all compositions have been determined at room temperature. These determinations have been made using an automatic hysteresis curve recorder in which the field strength, H , is automatically subtracted from the total induction, B , to yield $4\pi M$ the intrinsic magnetization.¹⁵⁾

13) Jonker, Wijn & Braun, Philips Tech. Rev. 18, 145-154 (1956/57).

14) Stuijts & Wijn, Philips Tech. Rev. 19, 209-217 (1957/58).

15) Brockman & Steneck, Philips Tech. Rev. 16, 79-87 (1954).

The observed intrinsic induction obtained in this manner was converted to the saturation per gram by the use of measured density of the specimen. The measured density was obtained from the volume, calculated from the linear dimensions, and the weight of the sample.

Alternatively, the observed intrinsic induction may be converted to the intrinsic induction at X-ray density by the use of the measured density and the X-ray density (q.v.).

Figure 4 shows graphically the experimentally determined values of the saturation per gram, σ , as a function of the substitution in the two series:



These σ values may be directly converted to saturations per unit volume at X-ray densities with simple reference to the X-ray densities.

(c) The Ratio $2K/M$

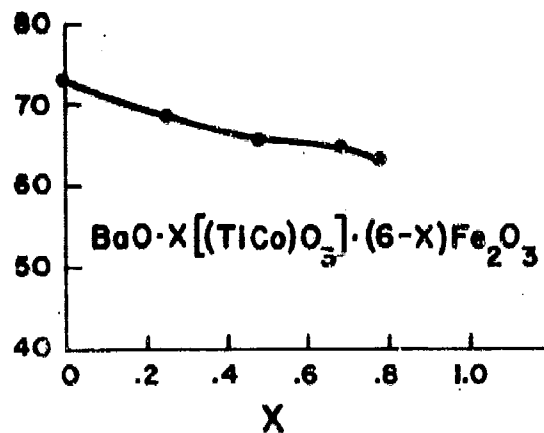
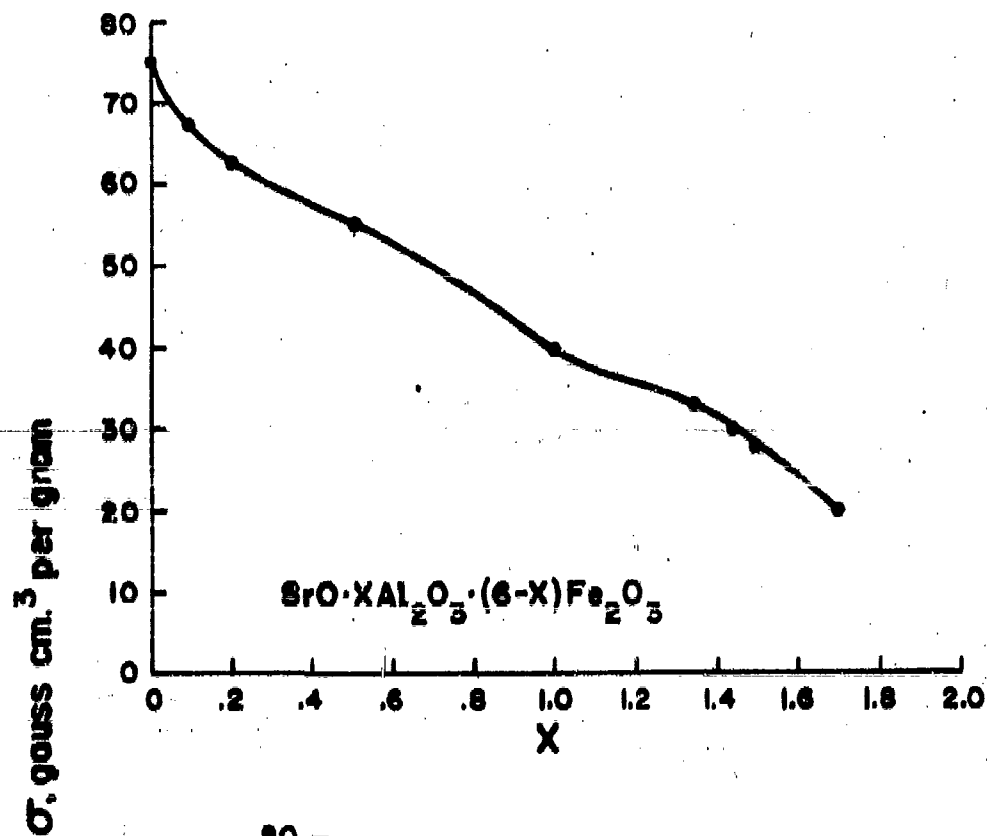
This ratio of the anisotropy constant to the saturation magnetization is of importance for two reasons:

1. The maximum theoretical intrinsic coercive force of a permanent magnet material (which may be described by the "fine-particle" picture) is directly related to this ratio.^{1,16,17)}

16) Bozorth, Elect. Eng. 68, 471-6 (1949).

17) Brockman, Elect. Eng. 71, 644-47 (1952).

Fig.4 SATURATION PER GRAM, σ
EXPERIMENTAL VALUES
(ROOM TEMPERATURE)



2. The internal or crystalline anisotropy field is given by this ratio, i.e. $H_{an} = 2K/M$. Ferro-magnetic resonance, due to this anisotropy field, is found to occur in the microwave region.

These two magnetic quantities are separately discussed in the following two sections.

(d) The Coercive Force

Van Uitert⁷⁾ has shown that the intrinsic coercive force of aluminum substituted $BaO \cdot 6Fe_2O_3$ and of aluminum substituted $SrO \cdot 6Fe_2O_3$ increases as the amount of aluminum replacing iron increases. This, in accordance with the fine-particle theory, implies that the ratio $2K/M$ should also increase as the aluminum content increases.

This increase in coercive force was also observed in this work. However, no effort was expended in trying to relate the coercive force to the amount of replacement. This was so because the coercive force is a structure sensitive magnetic property and may be varied over wide limits by various processing variables.

On the other hand, the diminishing anisotropy constant¹⁰⁾ associated with the replacement of iron by titanium-cobalt can be expected to lead to diminishing coercive forces. These are indeed the findings in this work. As a result, with the higher Ti-Co substitutions, the permanent magnet properties deteriorate.

As noted above, the coercive force is structure sensitive. We have investigated the possibility of increasing the coercive force of one of the Ti-Co materials. This is reported in our Report 29 (Table I). By altering the initial particle size of the powder and the firing conditions, it was found possible to vary the coercive force from over 1400 oersteds to 30 oersteds in the composition $\text{BaO} \cdot 0.48[(\text{TiCo})\text{O}_3] \cdot 5.52\text{Fe}_2\text{O}_3$. The larger coercive forces are obtained through a sacrifice in the final fired density, and therefore, perhaps, at a sacrifice in machinability.

(c) The Internal Field

Van Uitert⁷⁾ has suggested that the increase in $2K/M$ (implied by his observations of the increase in the coercive force accompanying an increased amount of aluminum replacing iron) should also cause ferromagnetic resonance to occur at frequencies greater than 50 kmc/sec (the natural resonance frequency of simple $\text{BaO} \cdot 6\text{Fe}_2\text{O}_3$). He cites a measurement by M. T. Weiss, in the frequency range of 50-56 kmc, confirming this suggestion.

The work reported here is a detailed study of the variation of the internal field (and therefore of the ferromagnetic resonance frequency) with the replacement of iron ion by aluminum ion in $\text{SrO} \cdot 6\text{Fe}_2\text{O}_3$. In addition, the decreasing internal field (and therefore the decreasing ferromagnetic resonance frequency) associated with the substitution of

titanium-cobalt in $\text{BaO} \cdot 6\text{Fe}_2\text{O}_3$ has been studied in detail.

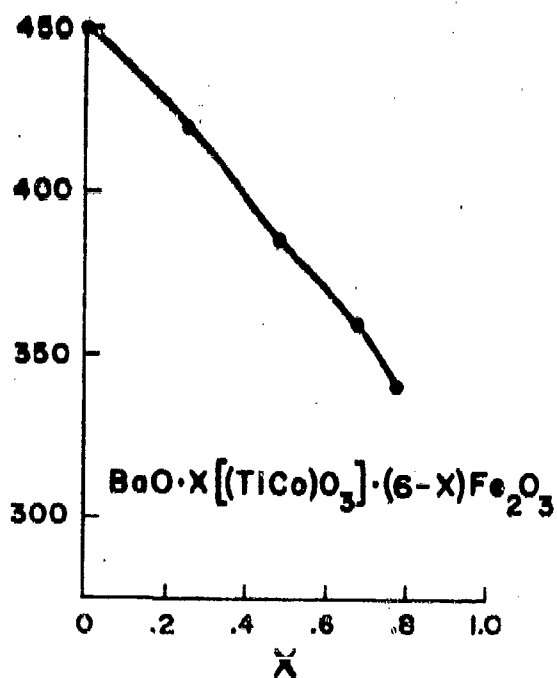
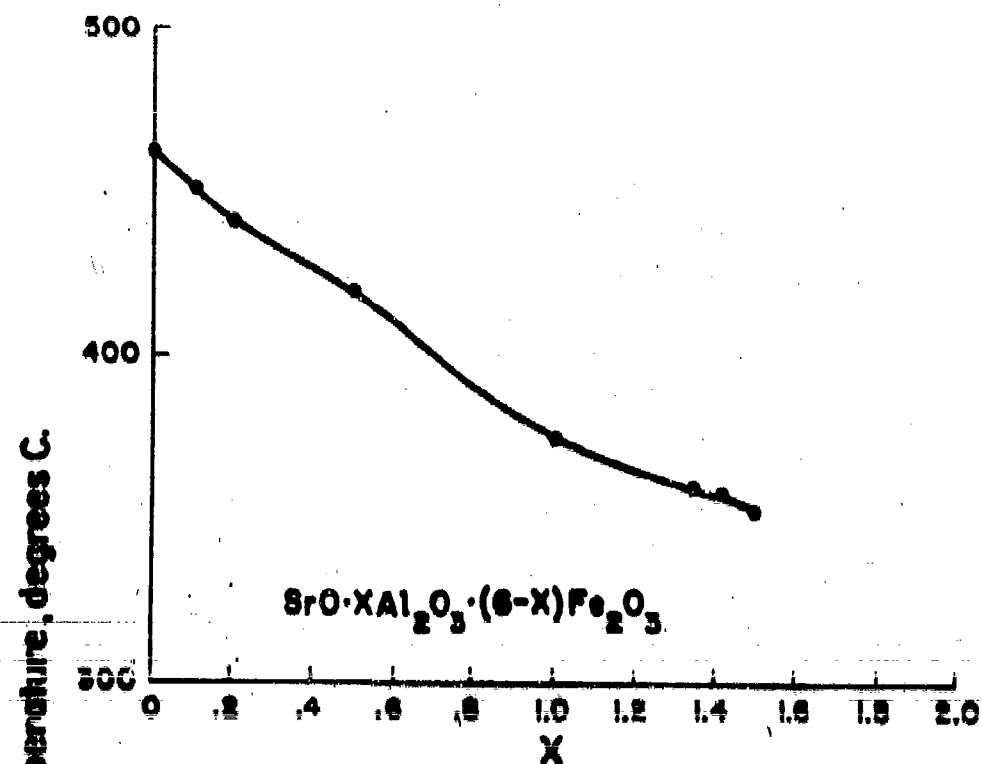
(f) The Curie Point

The Curie temperatures for the various compositions* have been determined. The variation of the remanent magnetism of a rod of the material in question with temperature served as a basis for the determination of the Curie temperature. The technique was described in Report No. 20 (Table I).

Figure 5 is a graphical representation of the experimental results.

* Lack of time prevented our determining the Curie temperature of the last aluminum substituted material: $\text{SrO} \cdot 1.7\text{Al}_2\text{O}_3 \cdot 4.3\text{Fe}_2\text{O}_3$.

Fig.5 CURIE TEMPERATURES
EXPERIMENTAL VALUES



V. Microwave Magnetic Properties

Introduction

Highly anisotropic magnetic materials can be useful at millimeter wavelengths because ferrimagnetic resonance can be made to occur in such materials with the application of little or no magnetic field. For example, in Ferroxdure ($\text{BaO} \cdot 6\text{Fe}_2\text{O}_3$) the high crystalline anisotropy causes an apparent magnetic anisotropy field along the hexagonal axis of 17.5 kilo-oersteds, resulting in a resonant frequency of about 50 kmc/sec with no externally applied magnetic field.^{18,19)} By adding to H_{an} an externally applied field, H_{ap} , the resonance can be made to occur at higher frequencies. However, there is a practical limit to this for to have the resonant frequency occur at 75 kmc/sec, the required value of H_{ap} for this material is about 10 kilo-oersteds. Thus, although this material is practical at M-band and even at R-band frequencies, it begins to be impractical at frequencies greater than 75 kmc/sec. Therefore, materials with a value of H_{an} higher than that of Ferroxdure are desirable for millimeter wave applications. Such materials have been obtained by a partial substitution of ferric ion by aluminum ion in $\text{BaO} \cdot 6\text{Fe}_2\text{O}_3$. For instance, in the series $\text{BaO} \cdot x\text{Al}_2\text{O}_3 \cdot (6-x)\text{Fe}_2\text{O}_3$, a variation of x from zero to unity increases H_{an} from 17.5 to about 28 kilo-oersteds. A similar effect was found to occur in the corresponding Sr series ($\text{SrO} \cdot x\text{Al}_2\text{O}_3 \cdot (6-x)\text{Fe}_2\text{O}_3$).

18) J. Smit and H. G. Beljers, Philips Res. Repts., Vol. 10, p. 113 (1955).

19) M. T. Weiss, Phys. Rev., Vol. 98, p. 925 (1955).

Of course, anisotropic materials can be useful at all frequencies where the applied field necessary for the resonance to occur is greater than that easily obtainable with a permanent magnet (say 7 kilo-oersteds). Therefore, it was also of practical interest to try to reduce the anisotropy field of Ferroxdure from its value of 17.5 down to about 7 kilo-oersteds. Such a continuous variation was found to be possible by varying x from zero to about 0.8 in the series²⁰⁾ $\text{BaO} \cdot x[(\text{TiCo})\text{O}_3] \cdot (6-x)\text{Fe}_2\text{O}_3$.

Experimental Procedure and Results

Figure 6 is a block diagram of the experimental arrangement. The power sources were commercially available klystrons, used directly or used to drive a harmonic generator. The corresponding diagram for the former case is found by eliminating the harmonic generator circuit.

The results of the microwave measurements are listed in the first two rows of Table IV. In this table, H_{an} is the room temperature anisotropy field, and ΔH is the room temperature linewidth of the ferrimagnetic resonance absorption line. Both H_{an} and ΔH were found from the measurement, at constant frequency, of microwave power transmission vs applied dc magnetic field, H_{ap} . The power transmission shows a minimum as a function of the applied field.

The samples were either E-plane or H-plane slabs in a waveguide with their preferred orientation always parallel to the rf E field; the dc magnetic field was also parallel to the E field and was always sufficient to keep the material magnetically saturated. A typical ferrimagnetic resonance line obtained in this manner for an H-plane slab of barium Ferroxdure is

20) E. W. Gorter, Colloque International de Magnetisme, Grenoble, 2-6 Juillet 1958, pp. 296-309.

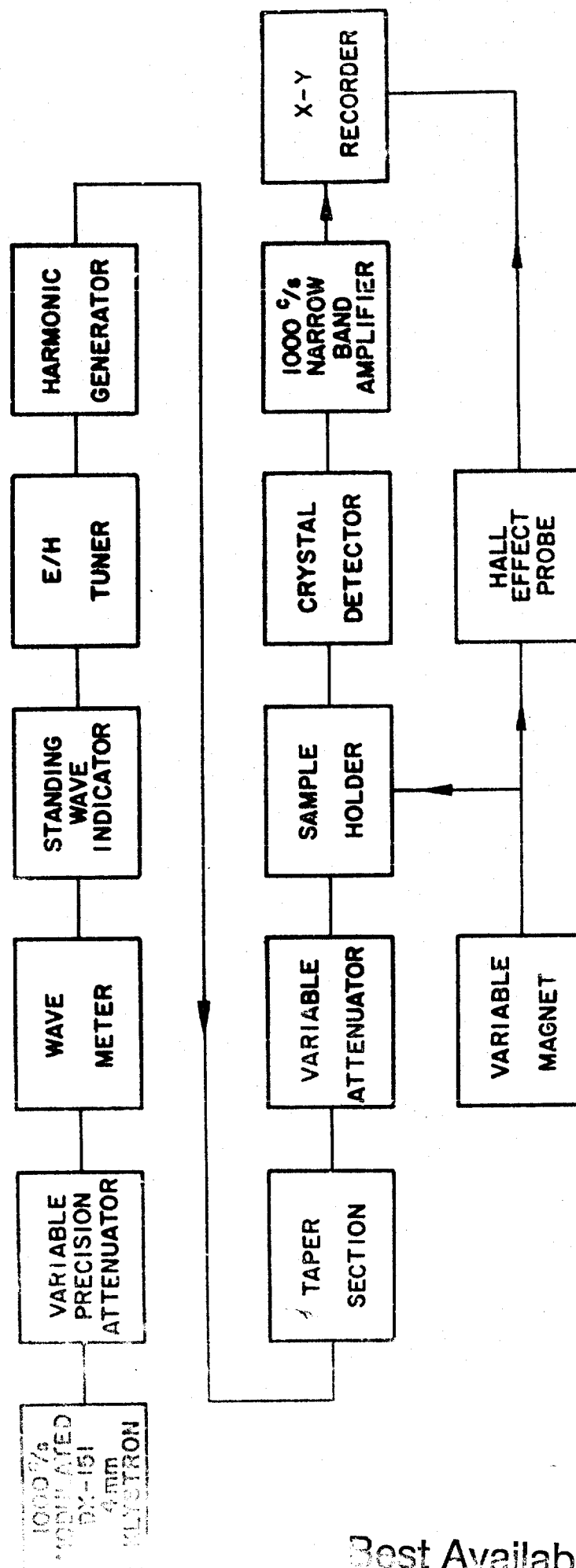


Fig. 6 BLOCK DIAGRAM OF MICRO-WAVE MEASUREMENTS CIRCUIT

TABLE IV

PROPERTIES OF THE MATERIALS INVESTIGATED

H_{an} = Anisotropy field in kilo-oersteds
 ΔH = Half-width of ferromagnetic absorption line in kilo-oersteds
 ν_{res} = No-field resonant frequency (for thin E-plane slab) in kmc/sec
 M = Saturation magnetization in kilogauss
 T_c = Curie temperature in $^{\circ}K$
 K = Anisotropy constant in 10^6 erg/cm³

	$Ba_{0.5-x}[(TiCo)O_3] \cdot (6-x)Fe_2O_3$				$BaO \cdot xAl_2O_3 \cdot (6-x)Fe_2O_3$		$SrO \cdot xAl_2O_3 \cdot (6-x)Fe_2O_3$								
x	0.78	0.68	0.48	0.25	0	1.0	0	0.1	0.2	0.5	1.0	1.35	1.42	1.50	1.70
H _{an}	6.55	8.75	11.5	14.8	17.5	28.1	19.3	20.2	20.8	23.4	31.0	40.6	42.1	44.3	53.4
ΔH	2.0	1.7	2.5	1.85	1.6	3.3	1.6	1.8	2.0	2.5	3.3	2.5	2.3	2.3	2.7
ν _{res}	23.0	29.3	36.7	45.8	53.1	78.2	57.8	59.6	61.0	67.1	86.2	111	115	121	145
4πM	4.25	4.35	4.4	4.6	4.9	2.2	4.8	4.3	4.0	3.5	2.5	2.0	1.8	1.7	1.2
T _c	614	633	658	693	723	625	737	725	715	694	648	605	605	600	---
K	1.11	1.51	2.01	2.71	3.41	2.46	3.69	3.46	3.31	3.26	3.08	3.23	3.02	3.00	2.55

shown in Fig. 7.

The value of the applied field at which the minimum transmission occurs, H_{ap}^{res} , is related to the frequency ν by Kittel's²¹⁾ formula for resonance:

$$\nu = \frac{\gamma}{2\pi} \left\{ [H_{an} + H_{ap} + (N_x - N_z)M] [H_{an} + H_{ap} + (N_y - N_z)M] \right\}^{\frac{1}{2}} \quad \text{Eq. (1)}$$

where N_x , N_y and N_z are the demagnetizing factors of the sample (considered as an ellipsoid) and the z direction is that of H_{ap} . In the derivation of Eq. (1) it is assumed that the size of the sample is much smaller than the wavelength. This, however, is seldom true in our experiments since we frequently use samples that are longer than the wavelength in the direction of propagation, so that a slow variation of the phase of the precession will occur along the sample. Nevertheless, it seems clear that one can still apply Eq. (1) as long as the demagnetizing coefficient in the direction of propagation is $\ll 1$, even if this coefficient is computed on the basis that the sample is only a half wavelength long.

The demagnetizing coefficients were estimated using Osborn's formula.²²⁾ By measuring H_{ap}^{res} at a number of different frequencies, both γ and H_{an} were obtained from Eq. (1). The room temperature values of $\gamma/2\pi$ turned out to be the same for all the compounds investigated, namely $\gamma/2\pi = 2.68$, corresponding to $g = \frac{2mc}{e} \gamma = 1.91$. (Similar measurements on single crystals gave $g = 1.96$.)

21) C. Kittel, Phys. Rev. 73, 155 (1948).

22) J. A. Osborn, Phys. Rev. 67, 351 (1945).

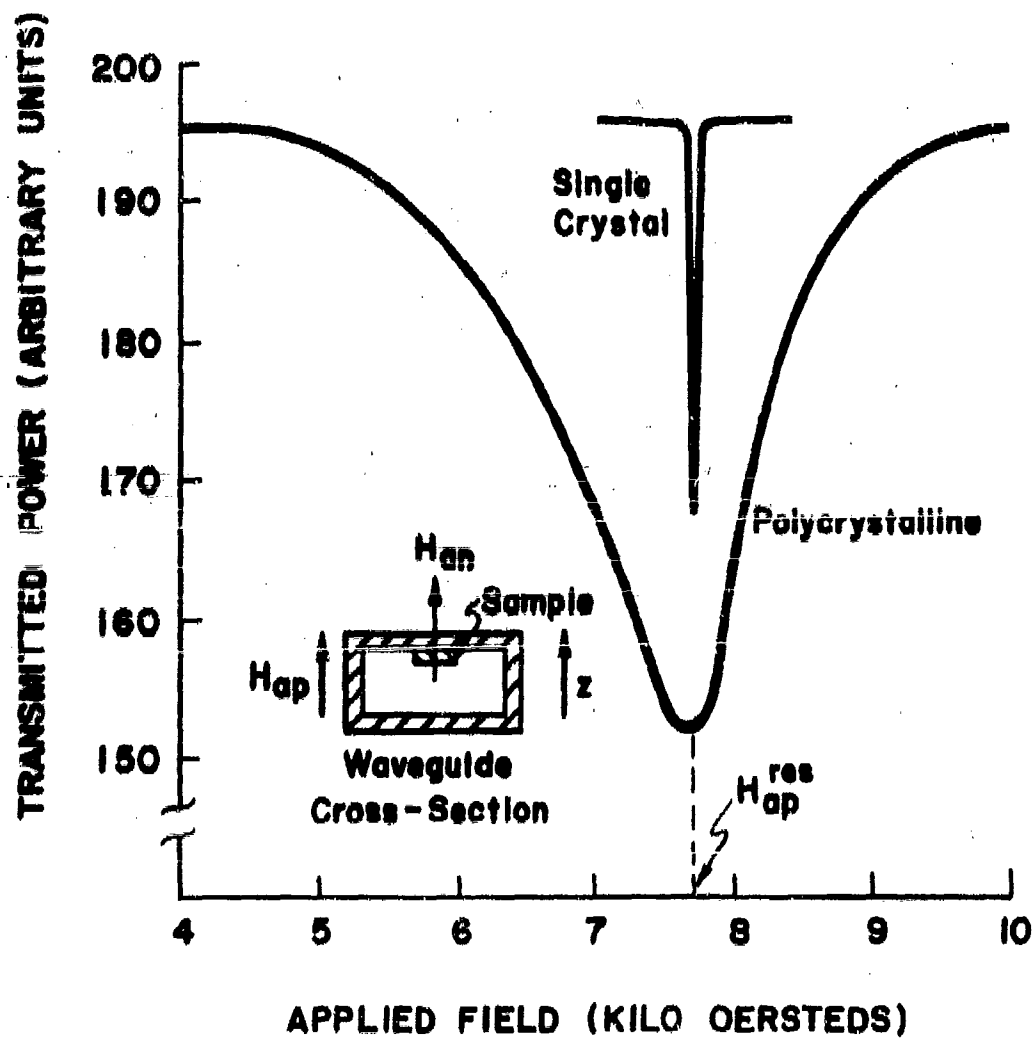


Fig. 7 A TYPICAL RESONANCE LINE FOR FERROXDURE
AT 57 kmc/sec

We should remark here that H_{ap}^{res} was determined with an accuracy of about 1%, and its value was found to be reproducible from sample to sample with about the same accuracy. The values of the frequency were determined to better than 0.3%. Therefore the computed values of H_{an} (which were always larger than H_{ap}^{res}) should have an accuracy of better than 1%.

The values of ΔH were obtained by measuring the line width at half the depth of the line on a "sufficiently thin" sample. A sample was considered sufficiently thin when the line width showed no further reduction with decreasing sample thickness. Thicknesses of about 0.001" were frequently required to satisfy this condition. Yet, as is clear from Fig. 7, the obtained linewidth cannot be considered an intrinsic property of the material as it is much larger than that of a single crystal of the same composition. We have not investigated the cause of the broadening of the line. However, it seems safe to assume that it is not due only to imperfect orientation of the crystallites, as measurements of the remanence in a direction perpendicular to the preferred one show that differences in orientation of different crystallites in the best samples are of the order of 5 degrees. Such small misalignments could not give rise to the broad lines observed in such samples. We might mention here that the linewidth decreases somewhat on prolonged firing of the samples, which also resulted in a noticeable increase in crystallite size. As the decrease in line width was considered too small to be of interest, no detailed investigation was made.

To illustrate how rapidly the natural resonant frequency varies

with H_{an} , and hence with composition, the resonant frequencies for the simple case $H_{ap} = 0$ were computed for very thin, long E-plane slabs (i.e. $N_x = N_z = 0$, $N_y = 4\pi$) from the experimentally determined values of H_{an} and are listed as ν_{res} in Table IV. For completeness, values of $4\pi M$, where M is the saturation magnetization, and of T_c , the Curie temperature, are also listed in the table. These quantities, apart from the units, are the same as those shown in Fig. 4 and Fig. 5. Finally, the table shows the values of the anisotropy constant as computed from the experimental microwave values of H_{an} and the experimental static values of M , using the formula $K = \frac{H_{an} \cdot M}{2}$.

Since, for the application in mind, the off-resonance microwave insertion losses of the material were of considerable importance, several compositions in the above-mentioned series were investigated for their insertion losses. Some of these investigations were forward loss measurements, i.e., transmission losses of long thin slabs positioned off center in a rectangular waveguide at the position of minimum absorption. In this procedure, it was assumed that most of the sample occupied a position of circular polarization opposite in sense to that required for resonance. During these measurements, the reverse loss, i.e., the resonance loss obtained with the direction of microwave propagation reversed in the above measurements, was also measured. This allowed an approximate check of the minimum isolator performance to be expected of these materials. The compositions thus investigated were $BaO \cdot 6Fe_2O_3$ and $x = 0, 0.2$ and 0.5 in the $SrO \cdot xAl_2O_3 \cdot (6-x)Fe_2O_3$ series; the measurements were made at M-band frequencies. Although the slabs in general were quite long ($\sim 2''$) and

of a nominal thickness ($0.006'' - 0.010''$), the forward insertion losses never exceeded 0.5 db.

Another type of loss investigation was of the background of the resonance line, near and far from resonance. In this procedure, a thin ($0.003''$), long ($2''$) magnetized H-plane slab was centrally located in the waveguide and the transmission (insertion) losses were measured with no applied field by the substitution method. $\text{SrO} \cdot 1.5\text{Al}_2\text{O}_3 \cdot 4.50\text{Fe}_2\text{O}_3$ was used for this investigation, its coercive force being so much larger than its $4\pi M$ that no difficulty was experienced with the sample demagnetizing, even in the zero applied field condition. The results of these measurements showed that the losses near but off resonance (in the 2 mm wavelength region), as well as the losses far from resonance (in the 4 mm wavelength region) were between 0.2 and 0.6 db.

Additional loss investigations were made in a manner similar to that above (i.e., centrally located slabs, substitution method) for various members in the (Ti + Co) substituted series and hence at lower frequencies (35-60 kmc/sec). Since the coercive forces of the members of this series were low ($< 4\pi M$), insertion loss measurements made away from resonance and with no applied fields almost invariably resulted in the complication of "low-field" losses.²³⁾ This complication was circumvented by going to frequencies slightly greater than $\gamma(H_{an} + 4\pi M)$ which, according to Smit and Polder, represents the maximum frequency at which a demagnetized sample would show losses of this type.²⁴⁾ Loss measurements

23) G. Rado, Rev. Mod. Phys. 25, no. 1, 81 (1953).

24) Smit and Polder, Rev. Mod. Phys. 25, no. 1, 89 (1953).

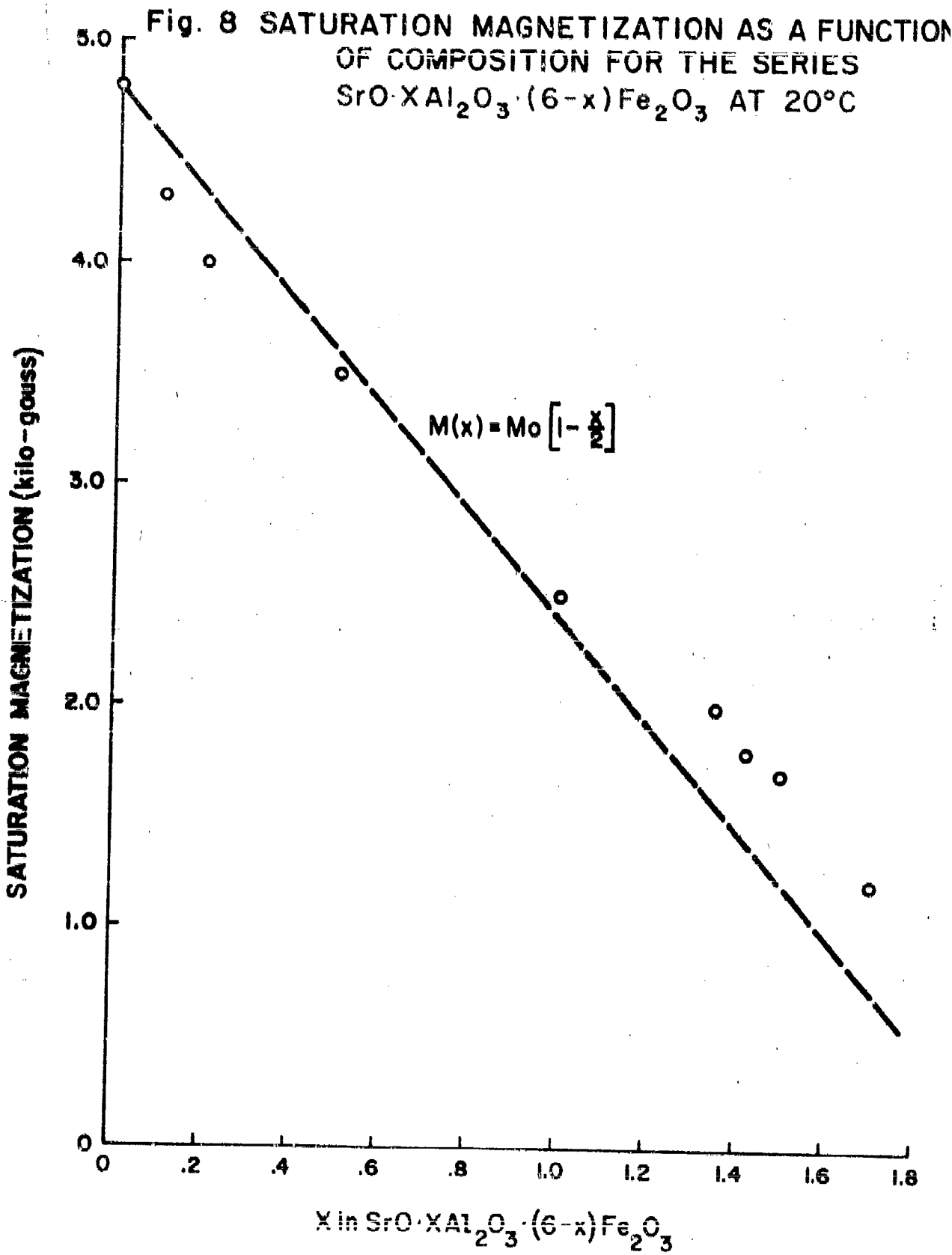
were generally made both below and above this frequency, and hence served to verify their expression for high anisotropy materials. The zero field insertion losses measured above this threshold frequency are considered to be the losses due to background of the resonance line, and hence are taken to be equal to the "forward" losses in the magnetized state. The resulting insertion losses obtained on H-plane slabs ($0.005''$ thick and $\geq 1.0''$ long) of the $x = 0.25, 0.48$ and 0.68 compositions in the $\text{BaO} \cdot x[(\text{TiO}_2)_3] \cdot (6-x)\text{Fe}_2\text{O}_3$ series were ≤ 0.4 db. The values obtained on the latter two compositions were also checked by the reflection method, which is especially useful for very low loss measurements.

In view of the moderately low insertion losses obtained for the various compositions investigated, it would appear that these materials should in general be satisfactory resonance isolator elements.

Interpretation of the Results Based on a Simple Model

A. $\text{BaO} \cdot x\text{Al}_2\text{O}_3 \cdot (6-x)\text{Fe}_2\text{O}_3$ Series

The points in Fig. 8 show the experimental variation of $4\pi M$ with aluminum content x , where the values are those of Table IV. These values of $4\pi M$ up to $x = 1.0$ agree well with those of Van Uitert,⁷⁾ who also measured this quantity at room temperature. Our room temperature values of $4\pi M$ up to $x = 1.0$ are consistently about 30% lower than the true (0°K) saturation values, which were determined by Bertaut, Deschamps and Pauthenet.⁹⁾ The 30% difference between room temperature and true saturation values is, at least for $x = 0$, in agreement with the experimental dependence of $4\pi M$ upon temperature as determined by Went, Rathenau, Gorter and Van Oosterhout.¹⁾



Also shown in Fig. 8, as a dotted line, is a linear variation derived in the following manner: The crystal structure of the series of compounds under discussion is the magnetoplumbite structure, the unit cell of which contains two molecules.¹²⁾ The unit cell, in which no aluminum has been substituted, contains 24 Fe^{3+} moments, of which 16 point in one direction and 8 in the opposite direction, along the c axis.¹⁾ After Al substitution, we have on the average $24 - 4x$ moments per unit cell. At least for small values of x, the Al exclusively replaces some of the 16 favorably oriented moments.⁹⁾ Thus we then have $16 - 4x$ moments pointing in one direction along the c axis and 8 in the opposite direction, leaving $8 - 4x$ moments uncompensated. Hence, $M(x)$, the saturation moment per unit cell, is proportional to $8 - 4x$, i.e.,

$$\frac{M(x)}{M(0)} = \frac{8 - 4x}{8} = 1 - \frac{x}{2} \quad \text{Eq. (2)}$$

Ignoring the small change in the size of the unit cell²⁾ with x, the ratio of the magnetic moments per cm^3 is also given by this linear relation, which is plotted as the dotted line in Fig. 8. Up to values of x of about unity, the agreement with the experimental points is fair. For larger values of x the deviation of the experimental points from the dotted line becomes serious. This suggests that the substitution of the Al ions is not completely preferential. It should be noted that we have used Eq. (2), which was derived for the true saturation magnetization, to compute the variation of room temperature values. It was surprising to us that the agreement was as good as that which we obtained using the true saturation values of Bertaut et al.⁹⁾

The solid line in Fig. 9 shows the smoothed experimental variation of H_{an} with aluminum content x , where the points shown are those of Table IV. Also shown, as a dotted line, is a theoretical variation derived in the following manner: The anisotropy field for magnetic materials with a preferred direction of the magnetization is given by the formula

$$H_{an} = \frac{2K}{M} \quad \text{Eq. (3)}$$

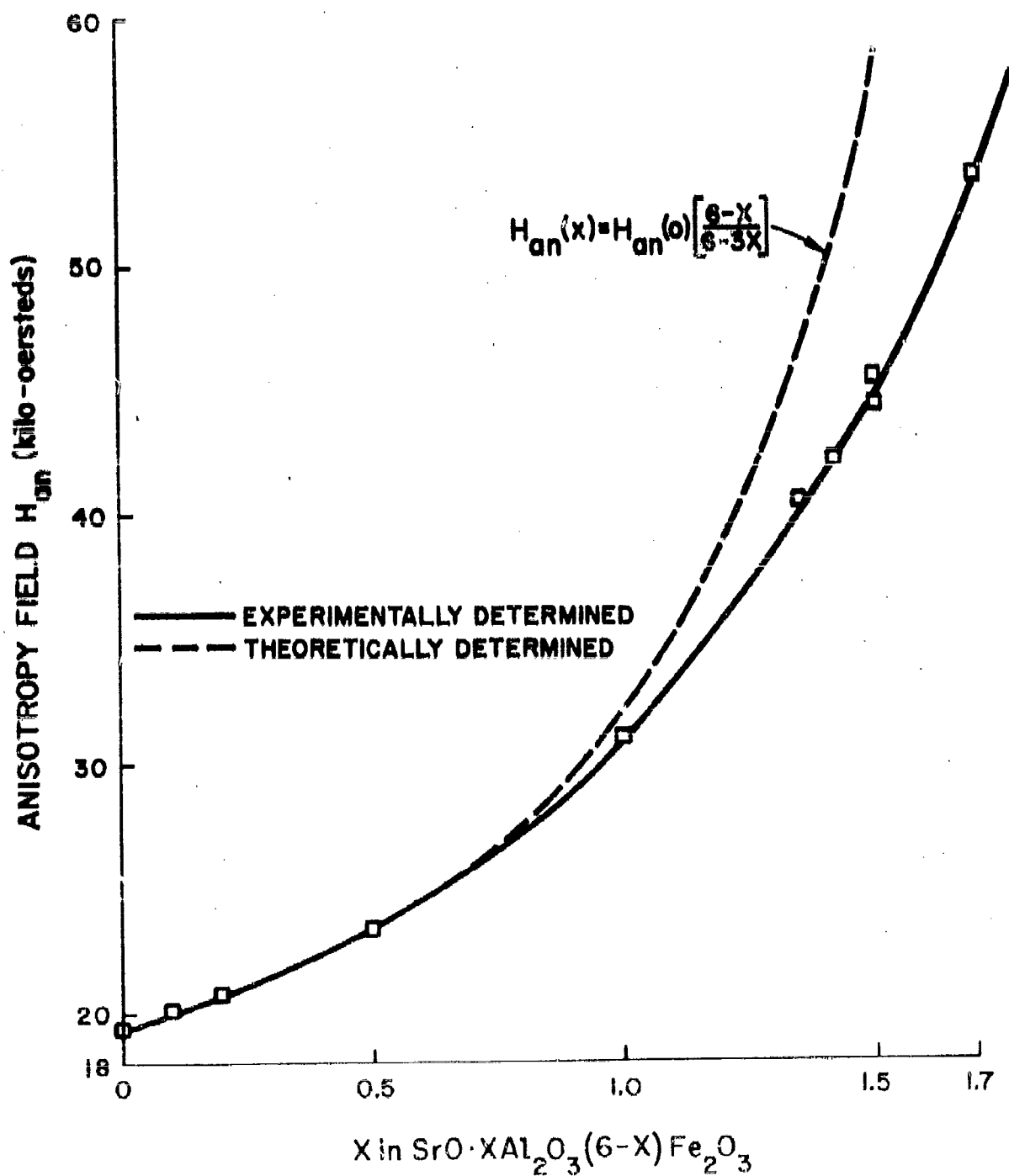
In the previous discussion, M and K were defined as the magnetization and the anisotropy constant per cm^3 . Ignoring once again the small changes in the unit cell dimension with composition, we can also take M to be the sum of the uncompensated moments per unit cell, and K to be the anisotropy constant per unit cell. We might remark here that, in agreement with its previous definition, K may also be defined by the relation that $2K\theta$ equals the restoring torque on all the moments per unit cell when they deviate by the small angle θ from the c direction.

Since in the above expression for H_{an} we already have an expression for the variation of M with x , an expression for the variation of K with x will give us $H_{an}(x)$. We propose to take K proportional to the total number of moments per cell, i.e., proportional to $24 - 4x$. We then obtain for the ratio of the anisotropy field in the compound with x moles of Al_2O_3 to that in the compound without Al_2O_3 :

$$\frac{H_{an}(x)}{H_{an}(0)} = \frac{6-x}{6-3x} \quad \text{Eq. (4)}$$

The dotted line in Fig. 9 is a plot of this relation, where $H_{an}(0)$ is taken to be equal to the experimental value. The agreement with the

Fig. 9 VARIATION OF THE ANISOTROPY FIELD WITH COMPOSITION IN $\text{SrO} \cdot X\text{Al}_2\text{O}_3(6-x)\text{Fe}_2\text{O}_3$



experimental curve is fair up to $x \approx 1.0$. At larger values the lack of agreement becomes considerable, but this is not surprising since the expression for $M(x)$ did not give a good fit to the experimental values for $x > 1.0$.

Returning to the anisotropy constant K , we rewrite Eq. (3) in the following form:

$$K(x) = \frac{H_{an}(x) M(x)}{2} \quad \text{Eq. (5)}$$

Since we have experimentally determined several values of H_{an} and M over the range of x from 0 to 1.7, we can compute $K(x)$ at these points, using Eq. (5). Values of $K(x)$ computed in this manner are plotted as the points in Fig. 10. We are now in a position to test our previous hypothesis for $K(x)$ (which was independent of the hypothesis for $M(x)$). According to our hypothesis, K is proportional to $(6-x)$, and this dependence is shown as the dashed straight line in Fig. 10. Although several of the points deviate considerably from the straight line, this line seems to represent the trend of the variation of K with x fairly closely.

In Fig. 11 the points show the experimentally determined variation of the Curie temperature with aluminum content x , where the values are those of Table IV. Also shown in Fig. 11, as a dotted line, is a linear variation based on the following considerations: If the material is heated to a temperature above its Curie point, the spontaneous magnetization of the two oppositely oriented groups of moments will vanish and only an external field can then magnetize the material. Let a field H (applied along the c direction) produce a magnetization M_1 per unit cell in one group of moments and M_2 in the other. For very small H , each

Fig. 10 VARIATION OF THE ANISOTROPY CONSTANT
WITH COMPOSITION IN
 $\text{SrO} \cdot x\text{Al}_2\text{O}_3 \cdot (6-x)\text{Fe}_2\text{O}_3$

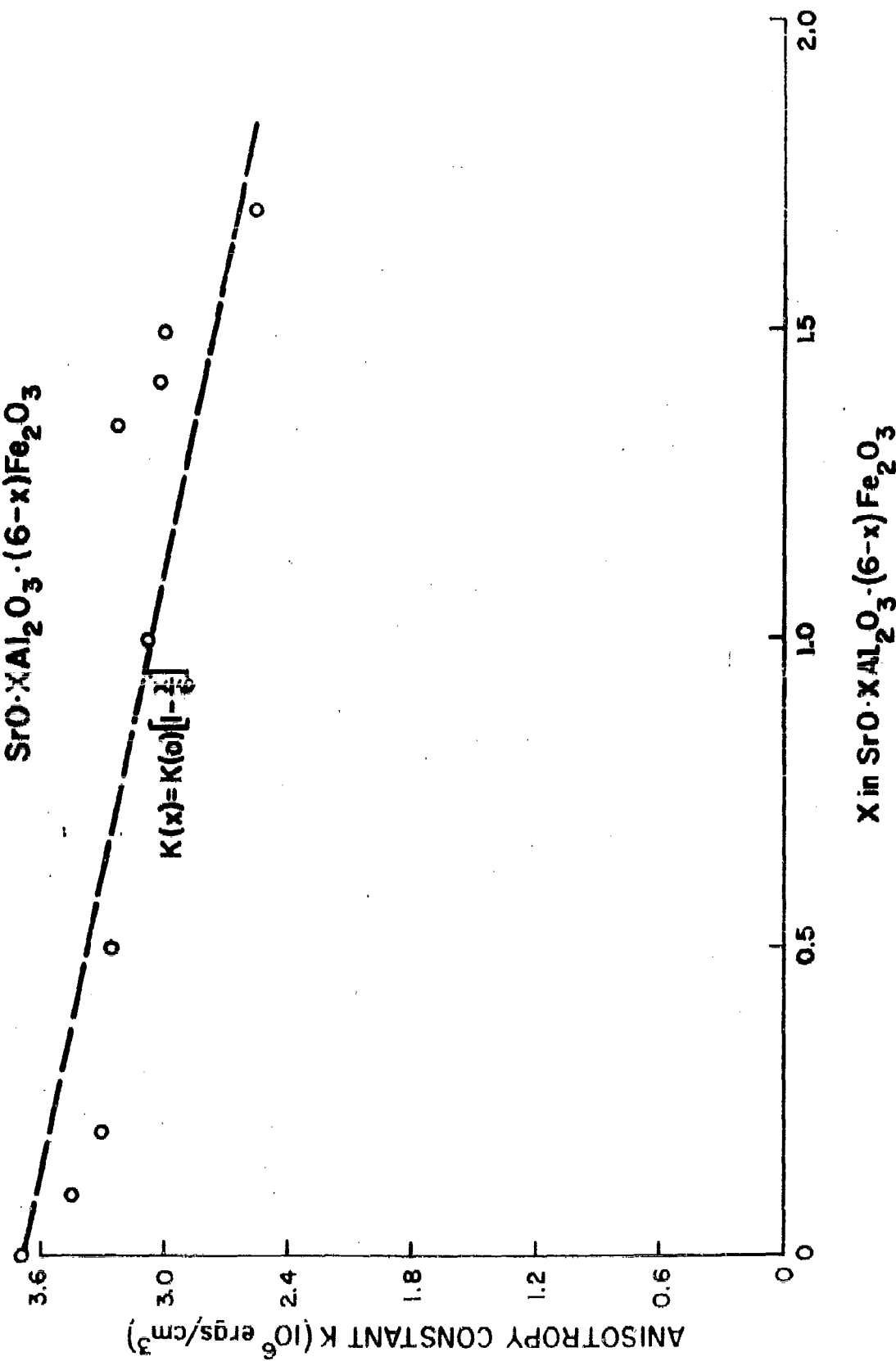
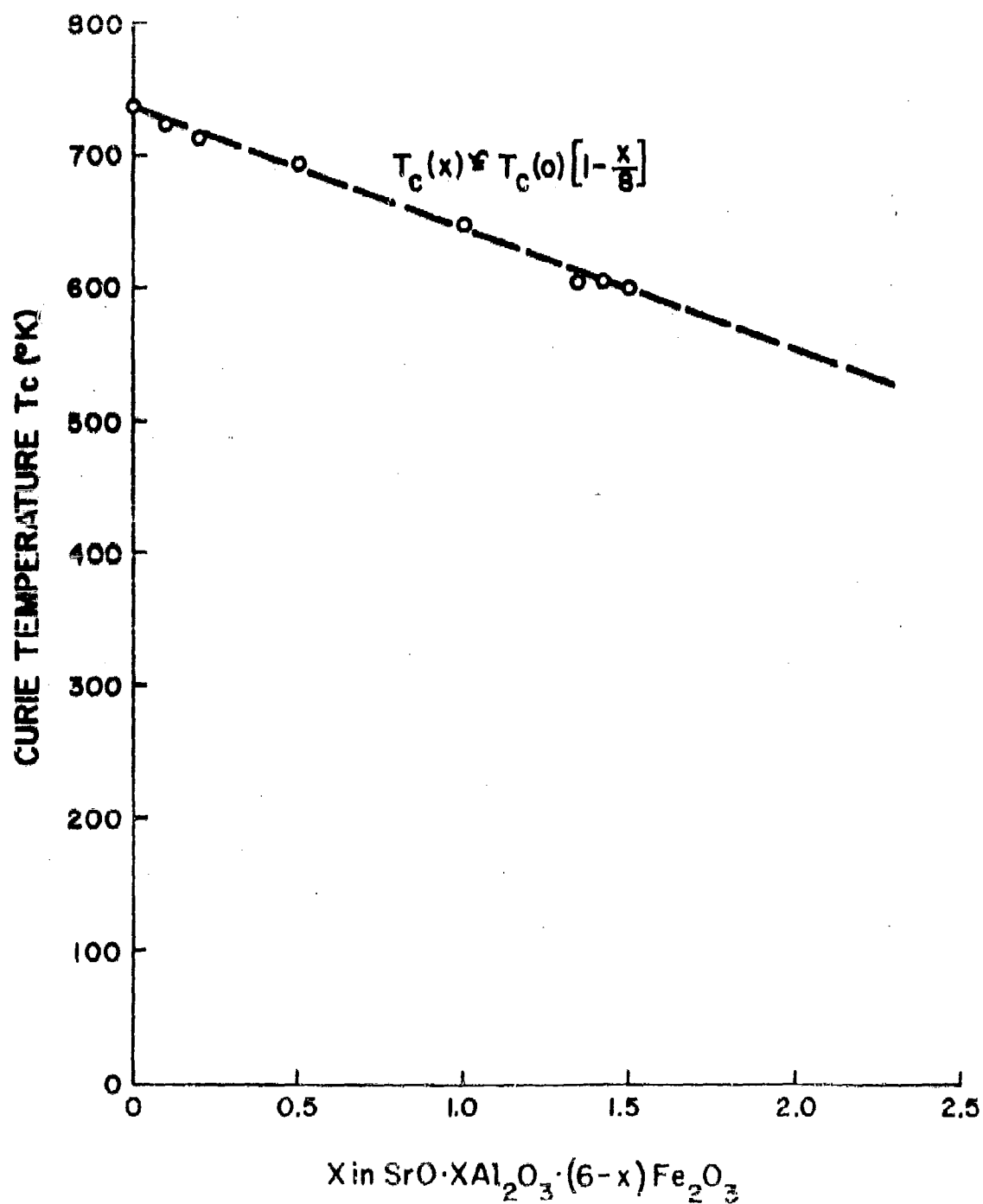


Fig. II CURIE TEMPERATURE vs. X FOR THE SERIES
 $\text{SrO} \cdot x\text{Al}_2\text{O}_3 \cdot (6-x)\text{Fe}_2\text{O}_3$



magnetization will be proportional to the effective field that each group feels. The effective field in a given group is assumed to be the sum of the applied field and the Weiss internal field due to the magnetization of the other group, which is the simplest of the cases considered by Neel.²⁵⁾ Furthermore, the magnetizations M_1 and M_2 are proportional to C_1/T and C_2/T respectively, where C_1 and C_2 are the respective Curie constants per cell. Thus, above the Curie temperature we have:

$$M_1 = \frac{C_1}{T} (H - N M_2) ,$$

$$M_2 = \frac{C_2}{T} (H - N M_1) ,$$

where N is the Weiss constant. For $H = 0$ these equations have only the trivial solution $M_1 = M_2 = 0$. If we now lower the value of T until these equations just have a non-zero solution for $H = 0$ (the threshold for spontaneous magnetization), we will have reached the Curie temperature T_c . Thus T_c is found from the condition that there is a solution of*

$$M_1 + \frac{C_1 N}{T_c} M_2 = 0 ,$$

$$\frac{C_2 N}{T_c} M_1 + M_2 = 0 .$$

This condition is $T_c = N \sqrt{C_1 C_2}$. Since the Curie constants in each group are proportional to the respective total number of moments per cell, then

25) L. Neel, Ann. Phys., 3, 137 (1948).

* This method of obtaining the Curie temperature is patterned after J. H. Van Vleck.

G_1 is proportional to $16 - 4x$ and G_2 is proportional to 8, each with the same proportionality factor given by the moment per Fe^{3+} . We then find

$$\frac{T_c(x)}{T_c(0)} = \sqrt{\frac{(16 - 4x) 3}{(16) 8}} = \sqrt{1 - \frac{x}{4}} \approx 1 - \frac{x}{8} \quad \text{Eq. (6)}$$

The dotted line in Fig. 11 shows the linear dependence of T_c upon x given by Eq. (6). This straight line fits the experimental points surprisingly well.

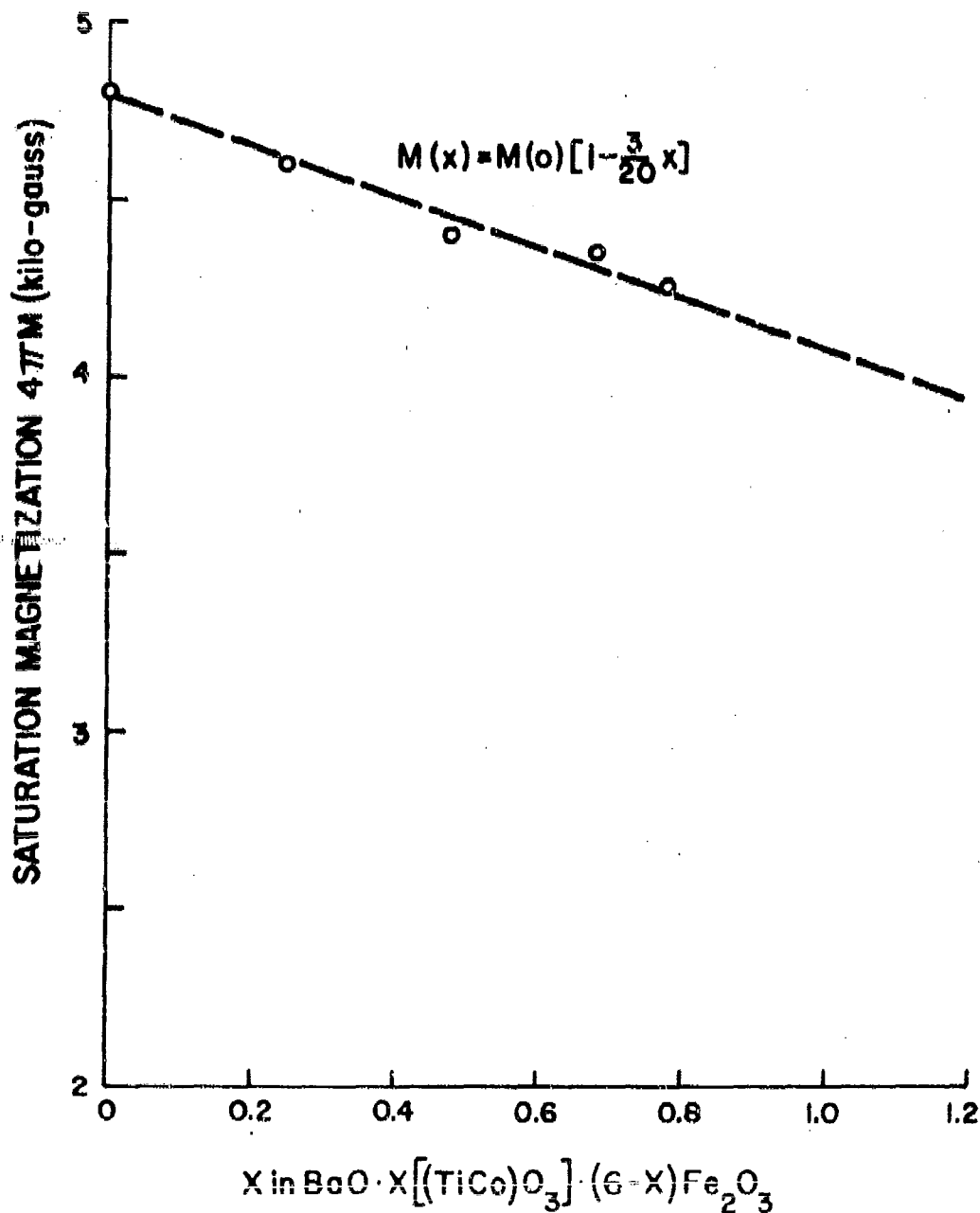
B. $BaO \cdot x[(TiCo)O_3] \cdot (6-x)Fe_2O_3$ Series

The points in Fig. 12 show the experimental variation of $4\pi M$ with $(Ti + Co)$ content x , where the values are those of Table IV. Our values are somewhat higher than the few points reported by Smit and Wijn.¹⁰⁾

Also shown in Fig. 12, as a dotted line, is a linear variation based on the assumption of a preferential substitution of the Ti and Co ions, similar to the one used in the previous case. We assume that the Ti ions exclusively replace some of the 16 favorably oriented moments (A-sites), and the Co ions replace exclusively some of the 8 other moments (B-sites). As the Co ions have 3 spins and replace Fe ions with 5 spins, each such replacement reduces the moment on a given site by $\frac{2}{5}$ of its original value. We thus have that the favorable moments per cell are reduced to the value $16 - 2x$, and the unfavorable ones to $8 - \left(\frac{2}{5}\right)2x$, leaving $8 - \frac{6}{5}x$ moments uncompensated. Hence, $M(x)$, the saturation moment per unit cell, is proportional to $8 - \frac{6}{5}x$, i.e.

$$\frac{M(x)}{M(0)} = \frac{8 - \frac{6}{5}x}{8} = 1 - \frac{3}{20}x \quad \text{Eq. (7)}$$

Fig. 12 SATURATION MAGNETIZATION AS A FUNCTION
OF COMPOSITION FOR THE SERIES
 $\text{BaO} \cdot x[(\text{TiCo})\text{O}_3] \cdot (6-x)\text{Fe}_2\text{O}_3$ AT 20°C



Ignoring the change in the size of the unit cell with x , the ratio of the magnetic moments per cm^3 is also given by this linear relation, which is plotted as the dotted line in Fig. 12. The agreement with the experimental values is quite good.

The points in Fig. 13 show the experimental variation of H_{an} with $(\text{Ti} + \text{Co})$ content x , where the values are those of Table IV. Also shown is a dotted curve, obtained by the following considerations:

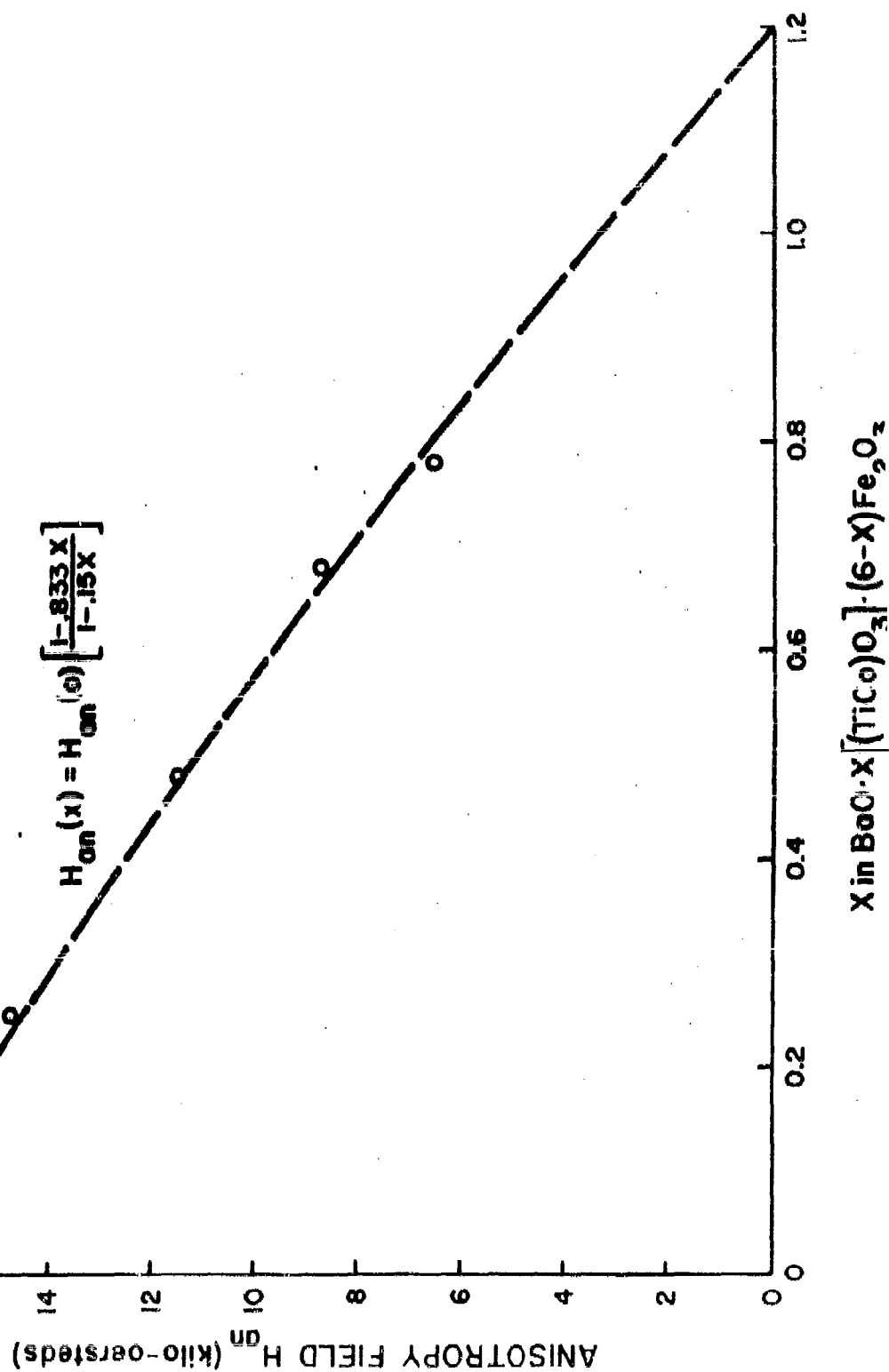
Since $H_{an}(x) = 2 K(x)/M(x)$, and since we already have an expression for $M(x)$, we need only an expression for $K(x)$ to obtain a theoretical expression for $H_{an}(x)$. We assume as before that each Fe^{3+} ion gives the same contribution to K . We make the same assumption for each Co^{2+} ion, although its contribution is not necessarily the same as that of the Fe ion. In fact, we shall assume its contribution to be equal to minus a times that of the Fe ion, where the actual value of a will be determined later. As we have in a unit cell $24 - 4x$ Fe ions and $2x$ Co ions, the anisotropy constant $K(x)$ becomes proportional to $24 - 4x + a(2x)$.

Combining this result with the one obtained above for $M(x)$, we find

$$\frac{H_{an}(x)}{H_{an}(0)} = \frac{1 - \frac{1}{12} (2 - a) x}{1 - \frac{3}{20} x} = \frac{1 - 0.833 x}{1 - 0.15 x} \quad \text{Eq. (8)}$$

The curve in Fig. 13 is obtained from this relation by choosing $a = -8.0$ in order to achieve a good fit with the experimental values. This large negative value of a shows the strong tendency of the Co spin to be oriented perpendicularly to the c axis (i.e., it displays planar anisotropy).

18 Fig. 13 VARIATION OF THE ANISOTROPY FIELD WITH COMPOSITION
IN THE SERIES $\text{BaO} \cdot x[\text{TiCoO}_3] \cdot (6-x)\text{Fe}_2\text{O}_3$



It is seen from the figure that the curve obtained in this manner predicts a vanishing anisotropy field for the composition $x = 1.2$.

Returning to the anisotropy constant K and using the formula $K = (1/2) H_{an} M$, several values of the anisotropy constant were obtained from the experimental microwave values of H_{an} and the experimental static values of M . These values are given in Table IV and are shown as the points in Fig. 14. Also shown, as a dotted line, is a linear variation of K which is obtained from our previous hypothesis that K was proportional to $24 - 4x + a(2x)$. Taking $a = -8$ we obtain from this expression

$$\frac{K(x)}{K(0)} = \frac{24 - 20x}{24} = 1 - \frac{5}{6} x. \quad \text{Eq. (9)}$$

This relation is plotted as the dotted line in Fig. 14. The agreement with the experimental points is quite good, and hence independently verifies our hypothesis of the linear decrease of K . Room temperature measurements reported by Smit and Wijn¹⁰⁾ do not indicate a linear variation of K with x . However, the present results agree with theirs at $x = 0$ and $x = 1.2$. Furthermore, recent measurements by Lotgering, Enz and Smit,²⁶⁾ which however were made at 90°K, also show a linear variation of K with x , their values being very similar to ours.

In Fig. 15 the points show the experimentally determined variation of the Curie temperature with (Ti + Co) content x , where the values

26) Lotgering, Enz and Smit, to be published in Philips Research Reports.

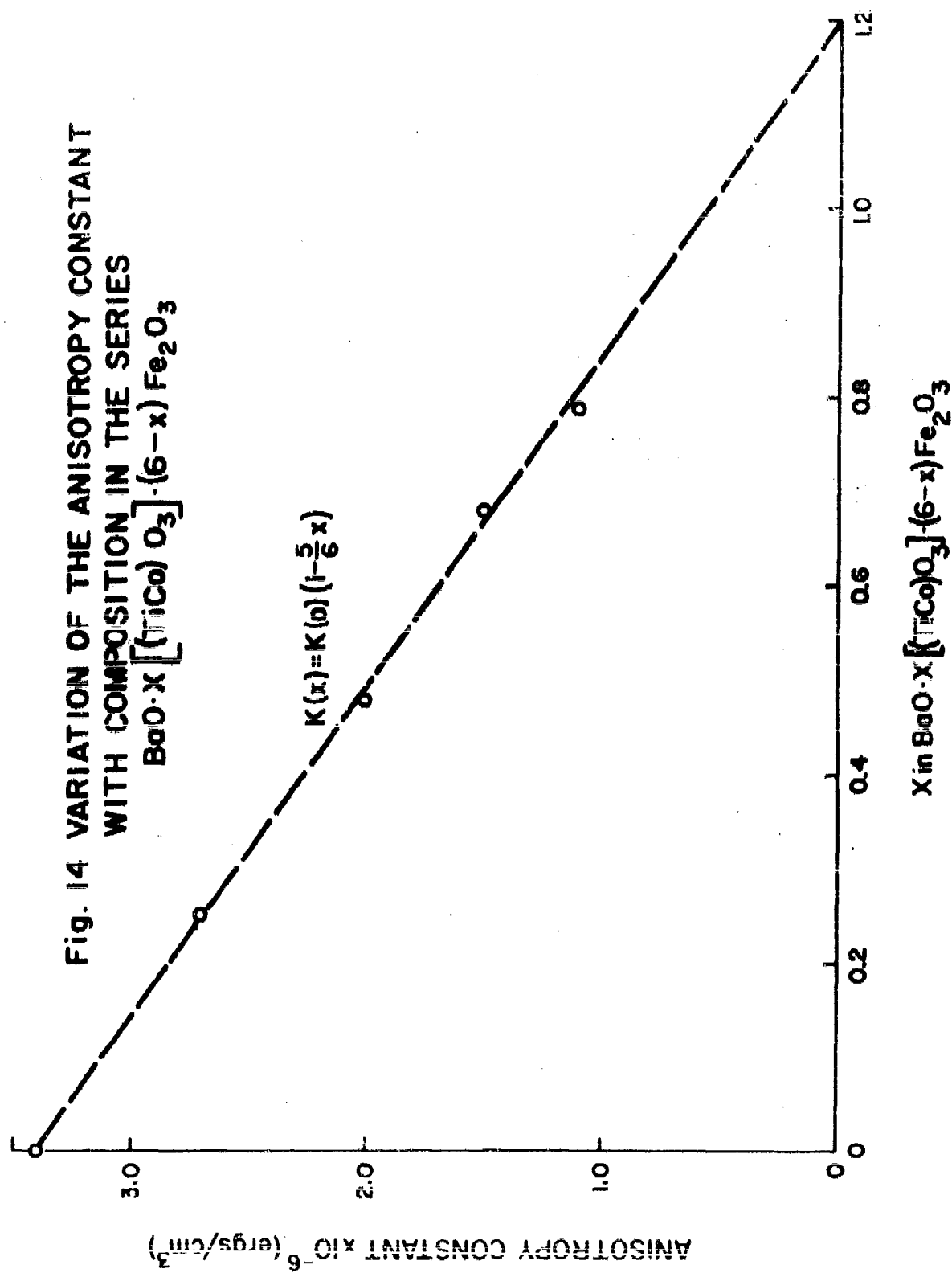
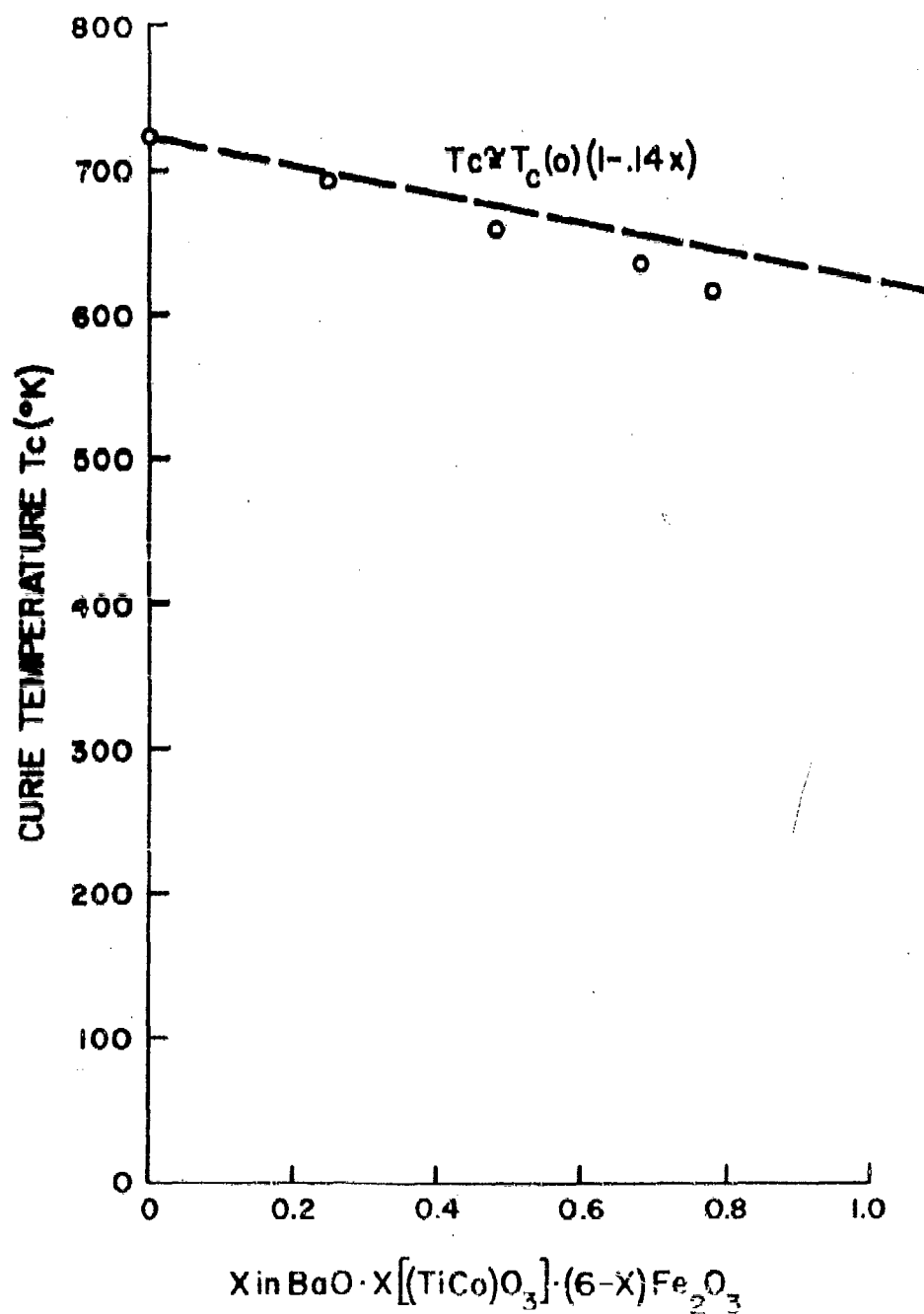


Fig. 15 CURIE TEMPERATURE vs. COMPOSITION FOR
THE SERIES $\text{BaO} \cdot x[(\text{TiCo})\text{O}_3] \cdot (6-x)\text{Fe}_2\text{O}_3$



are those of Table IV. Also shown in Fig. 15 is a dotted line arrived at by the following considerations: In the previously obtained formula $T_c = N\sqrt{C_1 C_2}$, where C_1 and C_2 are the Curie constants per cell of the two groups of magnetic ions. Since the Curie constant of a group of magnetic ions is proportional to the product of the total number of ions and the square of the moment per ion,* and again assuming that the Co ions replace exclusively some of the Fe moments in the B-sites, we find

$$C_1 \sim (16 - 2x) (1)^2 = 16 - 2x ,$$

$$C_2 \sim (8 - 2x) (1)^2 + 2x\left(\frac{3}{2}\right)^2 = 8 - \frac{32}{25} x .$$

In the same manner as before, we then find

$$\frac{T_c(x)}{T_c(0)} = \sqrt{\frac{16 - 2x}{16} \cdot \frac{8 - \frac{32}{25}x}{8}} \approx 1 - 0.14 x . \quad \text{Eq. (10)}$$

The dotted line in Fig. 15 shows the linear dependence of T_c upon x given by this equation. Although the fit to the experimental points is not as good as in the previous case, it is still considered satisfactory.

VI. Some Remarks on Single Crystal Measurements

Although most of the work reported here was done on polycrystalline materials, a few single crystals that were available were investigated for comparison. The compositions of these single crystals were

* Actually the ratio of the magnetic moments is not given by the ratio of the spins S , but by $10)$ the ratio of the quantities $\sqrt{S(S+1)}$. We have ignored these small differences in this approximate theory.

$\text{BaO} \cdot 6\text{Fe}_2\text{O}_3$, $\text{BaO} \cdot 0.2\text{Al}_2\text{O}_3 \cdot 5.8\text{Fe}_2\text{O}_3$ (both obtained from USASRDL) and $\text{SrO} \cdot 0.45\text{Al}_2\text{O}_3 \cdot 5.55\text{Fe}_2\text{O}_3$ (obtained from the Philips Research Laboratories, Eindhoven).

The final measurements were performed on thin H-plane slabs at M-band frequencies. The observed ferrimagnetic resonance absorption lines were very narrow compared to those observed in the polycrystalline samples, but always showed some structure, i.e., the line actually consisted of a narrow group of lines. The samples were made as thin as possible to eliminate most of this structure, but even at the smallest practical thickness of 0.001" there was some residual structure left. Reduction of the thickness not only reduced the structure but also the width of the main line of the pattern. The minimum width of the main line was for each material about 50 oersteds. The average g-value for these materials was found to be 1.94 (whereas the polycrystalline materials had $g = 1.91$). The anisotropy fields for these single crystals were found to be identical to the anisotropy fields for the corresponding polycrystalline materials.

VII. Examples of the Application of the Aluminum Substituted Materials in Simple Resonance Isolators

The above discussed anisotropic magnetic materials are useful at millimeter wavelengths because ferrimagnetic resonance can be made to occur in such materials with the application of little or no magnetic field. One of the obvious applications is in microwave resonance isolators in the millimeter wave range where the use of isotropic materials would necessitate the application of strong external magnetic fields.

A few simple resonance isolators were constructed using oriented materials of the type described above. A discussion of the performances of some of these isolators follows. Two standard geometries were used, i.e., an E-plane slab or an H-plane slab placed off-center in M-band waveguide. The slabs were fabricated so that the preferred direction (direction of H_{an}) was parallel to the E direction in the guide. In view of the favorable demagnetization factor for an E-plane slab, little or no external magnetic field is necessary to keep the material saturated once it is fully magnetized in its preferred direction. Figure 16 shows a typical performance curve obtained for an E-plane isolator with no external field. The material used was the Br material with $x = 0.5$. The overall dimensions of the (composite) slab are 0.003" thick x 0.050" high x 0.960" long; it was composed of four shorter slabs glued end-to-end on a quartz backing strip 0.012" thick x 0.065" high x 1.24" long. The thickness of this backing strip was experimentally adjusted to position the magnetic material in the waveguide for maximum transmission in the forward direction at the center frequency of the device. The figure shows a reverse loss greater than 10 db over a 3 kmc/sec bandwidth; the forward losses are about 1 db with a VSWR of 1.1. The peak value of the ratio of the reverse to forward losses (R/F), both in db, is about 12. Comparable results were obtained without the quartz, which therefore contributed no useful dielectric loading but acted primarily as a spacer and as a heat path to the side wall. No attempt was made to improve the performance by further dielectric loading.

Figure 17 shows a cross section of the device used in deter-

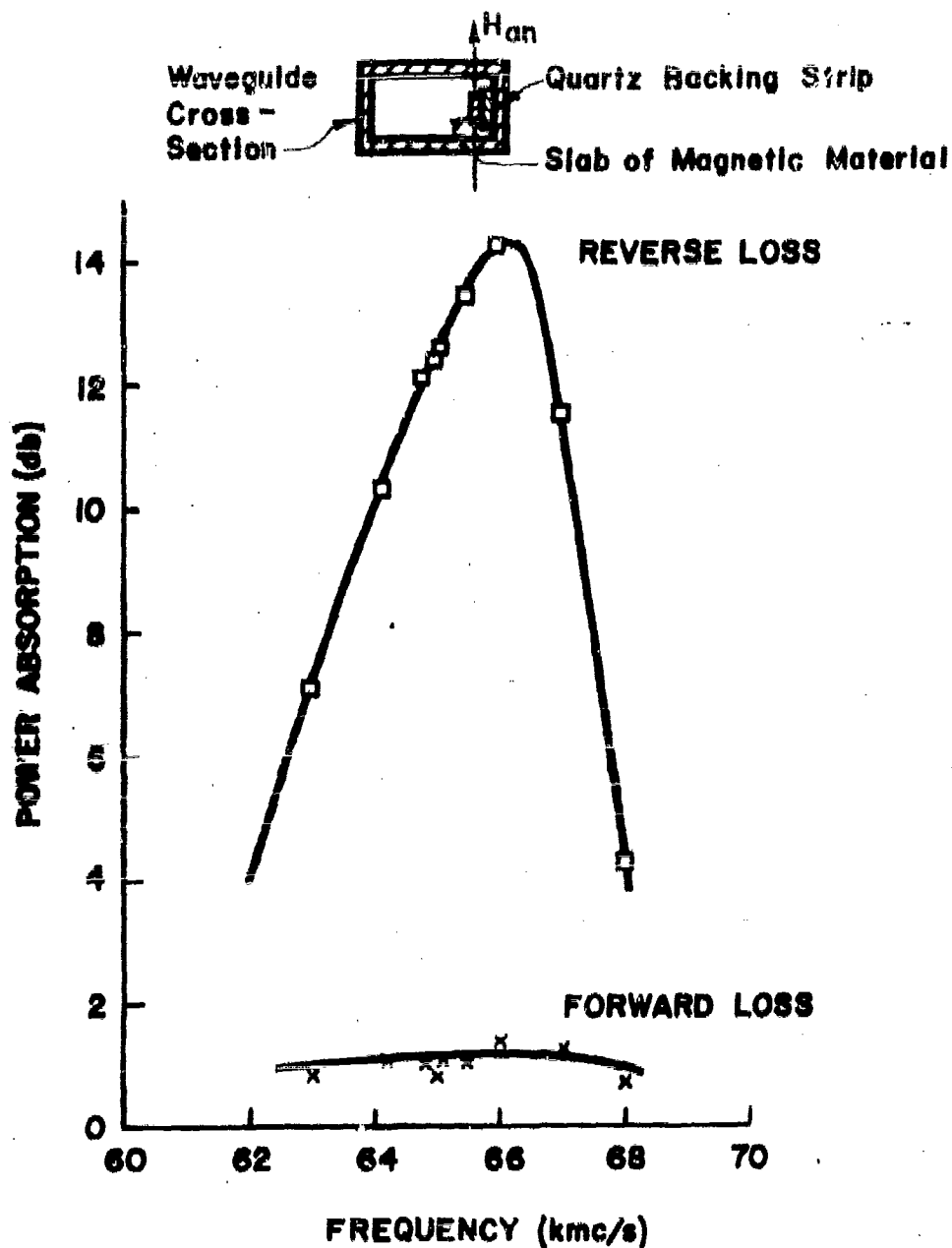


Fig. 16 REVERSE AND FORWARD LOSS MEASUREMENTS
OF AN E-PLANE ISOLATOR USING
 $\text{SrO} \cdot 0.5\text{Al}_2\text{O}_3 \cdot 5.5\text{Fe}_2\text{O}_3$
WITH NO EXTERNAL FIELD

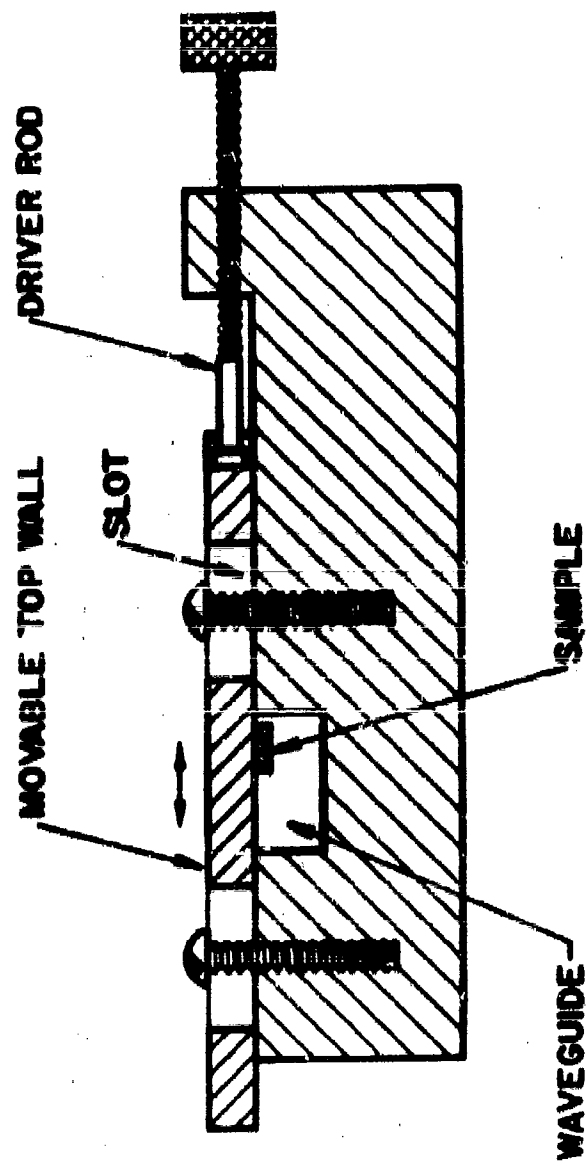


Fig. 17 WAVEGUIDE DEVICE FOR FORWARD AND REVERSE
ABSORPTION MEASUREMENTS

mining the performance of H-plane isolators. The waveguide was made by milling a groove in a copper block. The movable top wall of the waveguide holds the magnetic sample and facilitates its positioning for a maximum transmission in the forward direction at the center frequency of the device. After this position is determined, the screws are tightened and the absorption measurements are made at neighboring frequencies.

Figure 18 shows a typical performance curve for an H-plane slab (0.007" thick x 0.020" wide x 1.20" long) of the Sr material with $x = 0.2$ with an applied field of 4100 oersteds. Reverse losses greater than 11 db are maintained over a 3 kmc/sec bandwidth. The forward losses show a stepwise increase toward higher frequencies, being about 0.5 db at the lower end of the band and about 1.3 db at the upper end. This stepwise increase in the forward losses seems to be characteristic of H-plane slabs of these materials. In the region where the losses are low, the highest R/F ratios are obtained; the peak value of this ratio is about 20 in the unit described. Actually, the 0.5 db loss at the lower end is almost completely due to waveguide losses.

The above applied field was about the field necessary to prevent the sample from demagnetizing as a result of the strong demagnetizing field ($\sim 4\pi M$) that occurs in a slab magnetized perpendicular to its plane (H-plane geometry). In fact, most permanent magnet materials demagnetize in this unfavorable geometry. However, it has been found possible to prepare some of these materials with such high coercive forces that they do not demagnetize under these conditions.

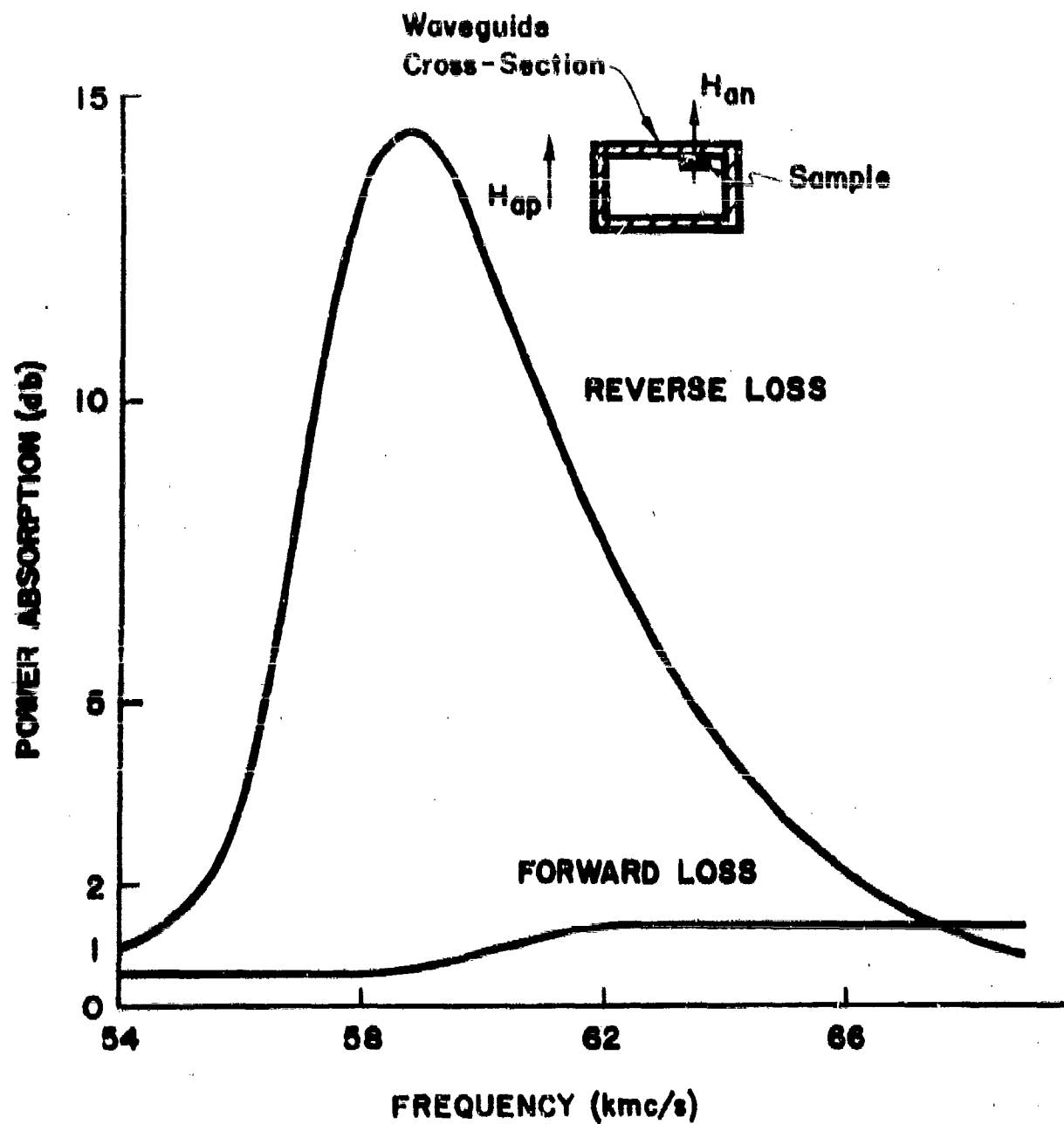


Fig. 18 REVERSE AND FORWARD LOSSES OF AN
H-PLANE SLAB OF $\text{SrO} \cdot 0.2\text{Al}_2\text{O}_3 \cdot 5.8\text{Fe}_2\text{O}_3$
WITH $H_{ap} = 4100$

For instance, the Sr materials for $x \geq 0.5$ show this unusual property. This suggested the possibility of constructing a resonance isolator using an H-plane slab of these materials which would require no applied field. Figure 19 shows a typical result of such a zero field configuration for the Sr material with $x = 0.5$. The slab is 0.008" thick x 0.020" wide x 1.20" long. A reverse loss of greater than 15 db is maintained over a 3 kmc/sec bandwidth, the forward loss being no greater than 1.2 db, with a VSWR of less than 1.1. The peak R/F value is 36. In general, the performance is as good as that of the applied field configuration.

Although the absorption lines of the materials under discussion are broad (see Table IV), additional broad-banding might still be desirable for certain applications. These tailor-made materials offer a novel method of attaining this end, i.e., by combining two (or more) materials of slightly different Al content with the attendant difference in natural resonance frequencies. Figure 20 shows the resulting performance of an isolator device combining the two Sr materials, $x = 0$ and $x = 0.2$, in a tandem arrangement of two H-plane slabs. Each slab is 0.007" thick x 0.020" wide x 0.50" long. The peaks of the individual resonance lines (reverse loss curve) are clearly resolved, with separation equal to that expected for these materials. A reverse loss of greater than 6 db is maintained over an 8 kmc/sec bandwidth. This performance shows promise for this method of broad-banding. The fact that the reverse losses are not very large is a consequence of the small amounts of the materials (half-inch long slabs) used in this preliminary design. The forward

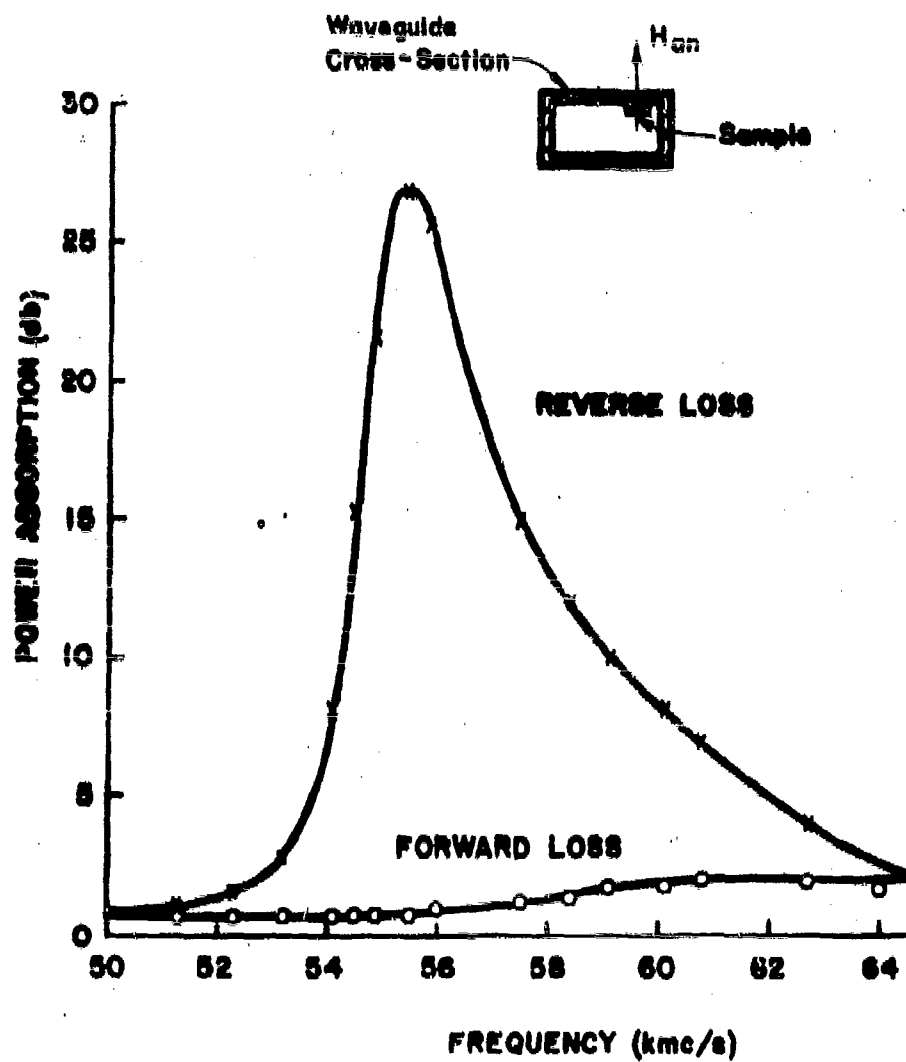


Fig. 19 REVERSE AND FORWARD LOSSES OF AN
H-PLANE SLAB OF $\text{SrO} \cdot 0.5\text{Al}_2\text{O}_3 \cdot 5.5\text{Fe}_2\text{O}_3$
WITH $H_{0p} = 0$

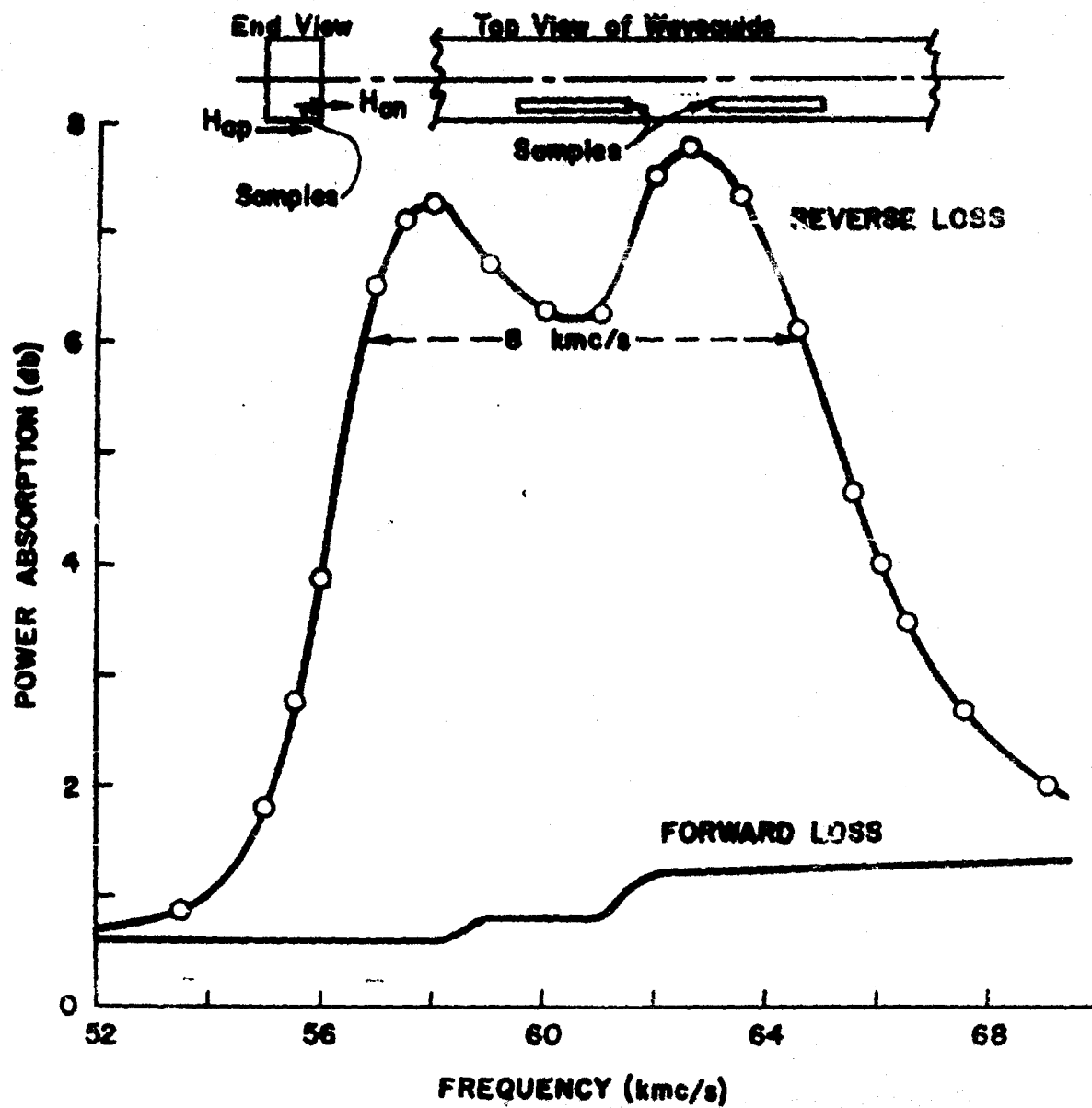


Fig. 20 REVERSE AND FORWARD LOSSES OF TWO H-PLANE SLABS OF SLIGHTLY DIFFERENT COMPOSITION, ARRANGED IN TANDEM.

$$H_{ap} = 5,800$$

Best Available Copy

losses are never greater than 1.3 db, and again show the stepwise increase toward the higher frequency end of the band. It should be pointed out that the performances of the various isolators described are expected to improve by dielectric loading. No such loading was attempted in the present work.

ENGINEERING SAMPLES SUPPLIED

UNDER CONTRACT NO. DA-36-039 SC-85279

Table V

Samples Prepared for Delivery under Contract, Refer to Transmittal Letter,
August 15, 1961

Our Sample Serial No.	Report No.* and page	Our Sample Serial No.	Report No.* and page
SrAlFe 8a5c2	#25 p. 10	BaTiFe 5a5c8	#30 p. **
SrAlFe 8a5c3	#25 p. 10	BaTiFe 5a5c9	#30 p. **
SrAlFe 8a6c1	#24 p. 10	BaTiFe 5a5c10	#30 p. **
SrAlFe 9a5c2	#24 p. 12	BaTiFe 6a5c2	#29 p. 14
SrAlFe 11a5c2	#29 p. 9	BaTiFe 6a5c3	#29 p. 14
SrAlFe 11a5c4	#30 p. **	BaTiFe 6a6c2	#29 p. 14
SrAlFe 11a6c1	#30 p. **	BaTiFe 6a7c2	#29 p. 14
BaTiFe 4a5c5	#26 p. 10	BaTiFe 6a7c3	#29 p. 14
BaTiFe 4a5c6	#26 p. 10	BaTiFe 7a5c1	#30 p. **
BaTiFe 4a6c1	#26 p. 10	BaTiFe 7a5c3	#30 p. **
BaTiFe 4a6c6	#26 p. 10	BaTiFe 7a6c3	#30 p. **

*Refer to Table I, Final Report, for cross reference of these report numbers
and contract quarterly or final reports.

**Report herewith.

Table VI

Listing of Samples Submitted under the Contract Prior to August 15, 1961

Refer to Transmittal Letter, August 15, 1961

Our Sample Serial No.	Report No.* and Page	Date of Transmittal	Method of Transmittal
BaTiFe 5a5c6	27 p. 9	1-25-61	In person by W.P.Arnett at Fort Monmouth.
BaTiFe 1a6c3	24 p. 14	5-10-61	In person to I.Bady at Irvington, N. Y.
BaTiFe 5a5c2	27 p. 9	5-10-61	In person to I.Bady at Irvington, N. Y.
BaTiFe 6a6c3	29 p. 14	5-10-61	For retransmittal to RCA personnel, per I. Bady.
BaTiFe 7a7c1	30 p. Q1	8-4-61	Letter of transmittal, D.J.DeBietto to L.Morris of RCA, dated 8-4-61, copy to I.Bady
BaTiFe 1a5 - .280T-1		1-24-61	Letter of transmittal, W.P.Arnett to I.Bady, 24 January 1961. These were oriented toroids, inside diameter 0.2". Refer to Report No. #28, p. 10 and "Final Report" together with "Sixth Quarterly Report" herewith.
BaTiFe 1a5 - .280T-2		1-24-61	
BaTiFe 1a5 - .280T-6		1-24-61	
BaTiFe 1a5 - .280T-7		1-24-61	
BaTiFe 1a5 - .280T-11		1-24-61	
BaTiFe 1a5 - .280T-13		1-24-61	
BaTiFe 1a5 - .280T-16		1-24-61	
BaTiFe 1a5 - .280T-17		1-24-61	
BaTiFe 1a5 - .280T-18		1-24-61	
BaTiFe 1a5 - .280T-20		1-24-61	
SrFe 21B10 - .280T-2		1-24-61	
BaTiFe 6a9 - 0.700T(2)-W-21		6-7-61	Letter of transmittal, F.G.Brockman to I.Bady, June 7, 1961. These were oriented toroids, inside diameter 0.5" (nominal). Refer to "Final Report" together with "Sixth Quarterly Report" herewith.
BaTiFe 6a9 - 0.700T(2)-W-24		6-7-61	
BaTiFe 6a9 - 0.700T(2)-W-25		6-7-61	
BaTiFe 6a9 - 0.700T(2)-W-29		6-7-61	
BaTiFe 6a9 - 0.700T(2)-W-32		6-7-61	
BaTiFe 6a9 - 0.700T(2)-W-33		6-7-61	
BaTiFe 6a9 - 0.700T(2)-W-37		6-7-61	
BaTiFe 6a9 - 0.700T(2)-W-38		6-7-61	
BaTiFe 6a9 - 0.700T(2)-W-43		6-7-61	
BaTiFe 6a9 - 0.700T(2)-W-44		6-7-61	

*Refer to Table I, Final Report, for cross reference of these report numbers and contract quarterly or final reports.

OVERALL CONCLUSIONS

The overall conclusion from the above work is that in the series $\text{SrO} \cdot x\text{Al}_2\text{O}_3 \cdot (6-x)\text{Fe}_2\text{O}_3$ the anisotropy field can be varied from about 19,000 to over 50,000 oersteds by a suitable choice of x between 0 and 1.7; similarly, in the series $\text{BaO} \cdot x[(\text{TiCo})\text{O}_3] \cdot (6-x)\text{Fe}_2\text{O}_3$ the anisotropy field can be varied from about 17,500 down to 7000 oersteds by a suitable choice of x between 0 and 0.78. These oriented hexaferrite materials have relatively low insertion losses away from their ferrimagnetic resonance, and are therefore potentially useful for the construction of broadband microwave resonance isolators in the frequency range of 25 to 150 kmc/sec. Furthermore, for those in the Al series of composition $x \geq 0.5$, it was found possible to construct H-plane isolators which required no external field to keep the material magnetized in this unfavorable geometry; these worked as well as those with a magnet. The linewidth of these oriented polycrystalline materials is of the order of 2000 oersteds, whereas that of the single crystal was found to be about 50 oersteds. The g -value of the polycrystalline version was found to be 1.91, whereas that of the single crystal was 1.94.

The simple models proposed to explain the variation of the saturation magnetization, the anisotropy constant, and the Curie temperature with composition for the two above-mentioned series appear in general to be fairly successful.

SIXTH QUARTERLY PROGRESS REPORT

15 April 1961 - 14 July 1961

ABSTRACT

This report gives in detail the work of the Sixth and Last Quarter of this Contract.

Tables are given for the permanent magnet properties of oriented samples made in this period.

The Curie temperature of $\text{BaO} \cdot 0.78 [(\text{TiCo})\text{O}_3] \cdot 5.22 \text{Fe}_2\text{O}_3$ is reported. The saturation magnetization of this material at room temperature is reported.

A discussion of circumferentially oriented toroids of $\text{BaO} \cdot 0.48 [(\text{TiCo})\text{O}_3] \cdot 5.52 \text{Fe}_2\text{O}_3$ is given.

Oriented polycrystalline slabs of $\text{BaO} \cdot 0.78 [(\text{TiCo})\text{O}_3] \cdot 5.22 \text{Fe}_2\text{O}_3$ were investigated in K and V microwave bands for their ferrimagnetic resonance. Several determinations of the crystalline anisotropy field were made; the resulting average value is 6550 oersteds. The observed linewidths were about 2000 oersteds. The measured g-value was found to be 1.91.

PROCEDURE, DATA AND RESULTS

Preparation and Properties of Oriented Magnetic Materials

(Refer to the accompanying Final Report for details of the processing and other details.)

1. Strontium Aluminum Ferric Oxide, $\text{SrO} \cdot 1.7\text{Al}_2\text{O}_3 \cdot 4.3\text{Fe}_2\text{O}_3$

In the Fourth Quarterly Progress Report, the control data for Preparation No. SrAlFe 11 of this composition were given for Step 8 of the processing procedure (see accompanying Final Report). The control data for this preparation at Steps 9 and 11 are given in Table Q-I.

The properties of oriented samples of this preparation were given in the Fifth Quarterly Progress Report, Table I. Some additional samples were prepared in this quarter. The permanent magnet properties of these additional samples are given in Table Q-II.

2. Barium Titanium Cobalt Ferric Oxide, $\text{BaO} \cdot 0.68[(\text{TiCo})\text{O}_3] \cdot 5.32\text{Fe}_2\text{O}_3$

The permanent magnet properties of oriented samples of this preparation were given in the Third Quarterly Progress Report, Table I. Some additional samples were prepared in this quarter. The permanent magnet properties of these additional samples are given in Table Q-III.

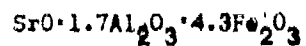
3. Barium Titanium Cobalt Ferric Oxide, $\text{BaO} \cdot 0.78[(\text{TiCo})\text{O}_3] \cdot 5.22\text{Fe}_2\text{O}_3$

The control data for this preparation are given in Table Q-IV.

The permanent magnet properties of oriented samples prepared are given in Table Q-V.

TABLE Q-I

CONTROL DATA FOR STRONTIUM ALUMINUM FERRIC OXIDE COMPOSITION



(Preparation No. SrAlFe 11)

Sample No.	Step*	Firing Temp. °C	Milling Time Hours	Density g/cc	B _R Gauss	B _{HC} Oe	γ _{HC} Oe
<u>SrAlFe</u>							
11a4R1	9	--	--	3.06	370	330	1980
11a5R1	11	--	29-1/2	2.94	330	300	3200
11a6R1	11	--	29-1/2	2.81	320	290	4330

* Refer to Fig. 2 of the accompanying Final Report for identification of phase of processing procedure.

TABLE Q-II

PERMANENT MAGNET PROPERTIES OF ORIENTED

SrO-Li₂OM₂O₃·4.3Fe₂O₃

(Preparation No. SrAlFe 11)

Sample	Sintering Temp. °C	Density G/cc	A. Parallel Direction				B. Perpendicular to A				D*	t_{90}/t_{10}	(BH)max Gauss- Oersteds
			orienting field		Br		Br		Br				
			B _g	B _H	B _g	B _H	B _g	B _H	B _g	B _H			
			Gauss	Oersteds	Gauss	Oersteds	Gauss	Oersteds	Gauss	Oersteds			
<u>SrAlFe</u>													
11a5C4	1418	4.48	1010	1000	5720	40	40	9900			See footnote	.333	.255 x 10 ⁶
11a6C1	1418	4.50	920	900	5820	90	90	7450			See footnote	.852	.21
11a6C2	1418	4.48	930	920	5850	90	90	8100			See footnote	.856	.22

$$* D = 1 - \frac{B_{r\perp}}{B_{r\parallel}}$$

Footnote: Very large field strengths are required to saturate this material in the difficult direction. Accordingly the perpendicular remanence is undoubtedly too low.

TABLE Q-III

PERMANENT MAGNET PROPERTIES OF ORIENTED



(Preparation No. BaTiFe5)

Sample	Sintering Temp. °C	Density G/cc	A. Parallel Direction orienting field				B. Perpendicular to A				D*	$\frac{l_{\parallel}}{l_{\perp}}$	(BH)max Gauss-Oersteds
			Br Gauss	H _C Oersteds	Br Gauss	H _C Oersteds	Br Gauss	H _C Oersteds	Br Gauss	H _C Oersteds			
<u>BaTiFe</u>													
5a5C7	1350	4.92	1730	60	250	110	180	180	0.144	0.856	0.819	--	
5a5C8	1350	4.90	1700	70	280	130	180	180	0.165	0.835	0.845	--	
5a5C9	1282	4.70	3390	140	290	170	370	370	0.085	0.915	0.766	0.18	
5a5C10	1282	4.78	2830	130	390	190	330	330	0.138	0.862	0.813	--	

$$* D = 1 - \frac{B_{r\perp}}{B_{r\parallel}}$$

TABLE Q-IV

CONTROL DATA FOR BARIUM TITANIUM-COBALT FERRIC OXIDE COMPOSITION



(Preparation No. BaTiFe7)

Sample No.	Step*	Firing Temp. °C	Milling Time Hours	Density G/cc	B _r Gauss	B ² C Oe	IHC Oe	Notes
<u>BaTiFe</u>								
7a3S1	8	1302	--	4.79	350	30	50	Fired alone 24 hrs. on temp.
7a3S2	8	1302	--	4.79	300	30	40	Fired with batch 24 hrs. on temp.
7a4R1	9	--	--	3.64	200	70	80	
7a5R1	11	--	12	3.23	450	130	170	
7a6R1	11	--	24	3.15	530	170	230	
7a7R1	11	--	50	3.01	650	220	300	

* Refer to Fig. 2 of the accompanying Final Report for identification of phase of processing procedure.

TABLE Q-V

PERMANENT MAGNET PROPERTIES OF ORIENTED



(Preparation No. BaLiFe7)

Sample	Sintering Temp. °C	Density G/cc	A. Parallel Direction orienting field				B. Perpendicular to A				$\frac{B_{\perp}}{B_{\parallel}}$	D*	$\frac{t_{\perp}}{t_{\parallel}}$	(BH)max Gauss-Cerstedts
			B_{\parallel} Gauss	B_{\parallel}^C Oerstedts	I_{\parallel}^C Oerstedts	B_{\perp} Gauss	B_{\perp}^C Oerstedts	I_{\perp}^C Oerstedts						
<u>BaLiFe</u>														
7a5C1	Unfired	2.90	730	120		130	190	100	200	.246	.754	1.00	--	
7a5C1	1251	4.41	1480	50		70	190	80	140	.128	.872	.877	--	
7a5C1a)	1251	4.48	1800	50		60	190	80	150	.105	.895	--	--	
7a5C2	1247	4.43	1480	60		70	190	80	150	.128	.872	.870	--	
7a5C3	1247	4.41	1570	60		70	200	80	160	.127	.873	.868	--	
7a6C1	Unfired	2.81	910	160		180	230	130	280	.253	.747	1.00	--	
7a6C1	1251	4.62	1760	60		60	230	100	180	.131	.869	.846	--	
7a6C1a)	1251	4.76	2380	60		60	230	100	170	.097	.903	--	--	
7a6C2b)	1200	4.02	1450	60		60	--	--	--	--	--	--	--	
7a6C3	1247	4.67	1920	60		70	230	120	180	.120	.880	.840	--	
7a7C1	Unfired	2.77	1120	220		250	310	180	370	.277	.723	1.00	--	
7a7C1	1251	4.65	2460	90		90	270	130	230	.110	.890	.827	--	
7a7C1a)	1251	4.78	3070	80		80	280	130	230	.091	.909	--	--	
7a7C2	1251	4.70	2500	80		90	280	130	230	.112	.888	.821	--	
7a7C2a)	1251	4.79	3000	80		80	280	130	230	.093	.907	--	--	

$$* D = 1 - \frac{B_{\perp}}{B_{\parallel}}$$

b) Rod shaped sample cut from oriented block with easy direction of orientation along cylindrical axis.

a) Results on samples after surface grinding.

4. Curie Temperature of $\text{BaO} \cdot 0.78 [(\text{TiCo})\text{O}_3] \cdot 5.22 \text{Fe}_2\text{O}_3$

The Curie temperature of this preparation was determined by the method mentioned in the accompanying Final Report.

$\text{BaO} \cdot 0.78 [(\text{TiCo})\text{O}_3] \cdot 5.22 \text{Fe}_2\text{O}_3$ Curie temperature, 341°C .

B. Saturation Magnetization

The saturation magnetization of $\text{BaO} \cdot 0.78 [(\text{TiCo})\text{O}_3] \cdot 5.22 \text{Fe}_2\text{O}_3$ was measured by the method referred to in the accompanying Final Report.

The observed room temperature saturation magnetization of $\text{BaO} \cdot 0.78 [(\text{TiCo})\text{O}_3] \cdot 5.22 \text{Fe}_2\text{O}_3$ was $47\text{M} = 3920$ gauss at a density of 4.93 g/cm^3 . This leads to a saturation per gram of $\sigma = 63$ gauss cm^3/g .

6. Circumferentially Oriented Toroids of $\text{BaO} \cdot 0.48 [(\text{TiCo})\text{O}_3] \cdot 5.52 \text{Fe}_2\text{O}_3$

(a) General Discussion and Fabrication

Melabs, Stanford Industrial Park, Palo Alto, Calif. requested, of the USASRDL, the fabrication of toroidally shaped samples of $\text{BaO} \cdot 0.48 [(\text{TiCo})\text{O}_3] \cdot 5.52 \text{Fe}_2\text{O}_3$ which should be oriented in the toroidal circumferential direction. Toroids of two sizes were required: (a) O.D. 0.25" I.D. 0.20" (b) O.D. 0.55" I.D. 0.50"; in either size, the suggested height was $1/4"$. The number of toroids of each size requested was 10.

As described in the accompanying Final Report, "Preparation of Anisotropic Samples", orientation of the fine powder (constituted

essentially of particles of single crystals) is accomplished by the application of a magnetic field having the direction of the desired direction of orientation.

Circumferential orientation of a toroid therefore requires the establishment of a circumferential magnetic field. The magnetic field surrounding a long straight current-carrying conductor is of this character. Indeed, this is the only obvious means of generating such a field. The die in which powder may be oriented and pressed to furnish a circumferentially oriented toroid would therefore be constructed so that an electric current could flow down the center arbor of the die. Then, in the annular space between the arbor and the cavity of the die, a circumferential magnetic field will be generated. The strength of the magnetic field about a current-carrying conductor varies inversely as the radial distance from the center of the conductor. Therefore the field is stronger at the center arbor and falls off by this inverse relationship across the annular space.

It is informative to estimate the current required to produce a given field at the inner surface of a cavity which could be used to press the larger of the two rings. The inside diameter of the cavity (the outside diameter of the pressed toroid) used to press these rings was 0.84" or 2.13 cm.* Since the field strength

*This was based on two considerations. First, the dimensional shrinkage upon firing, in the oriented direction, is roughly 40%. Second, the finished wall thickness of 0.025" (or 0.063 cm.) is too small to be fabricated directly. Since, in any event, Melabs intended to adjust the final dimensions by grinding, the O.D. and I.D. were chosen so that finished rings of about 1.53 cm O.D. and 1.23 cm I.D. were produced. This permitted adjustment of both O.D. and I.D.

is directly proportional to the current, it is convenient to calculate the current per 1,000 oersteds. At a radial distance of 1.06 cm (diameter 2.13 cm.) this current is 5,300 amperes per 1,000 oersteds.

Wijn^(Q1) studied the role of domain walls in Ferroxdure and in this study he used, among other samples, a circumferentially oriented toroid of $\text{BaO} \cdot 6 \text{Fe}_2\text{O}_3$. In this reference it is reported that the samples were prepared by Ir. A. L. Stuyts. In a private communication, Ir. Stuyts has kindly supplied us with the details of his experimental techniques. He made toroids of two sizes. The inside diameters of the cavities (the outside diameters of the pressed toroids) were about 0.7 cm in the one case and 2.0 cm in the other. For the 0.7 cm size, the orienting field was produced by a direct current of 2,500 amperes flowing through the center arbor of the die. For the larger toroids (2.0 cm) the orienting field was established by pulse techniques. A 9,600 microfarad (6 Kv rating) bank of condensers was charged to 2 Kv and then discharged through a Philips PL 5555 Ignitron. The discharge current was conducted through the center arbor of the die to produce the orienting field. The discharge current was estimated to be about 7000 to 8000 amperes.

Both of the two systems above represent rather formidable equipment requirements. At the time of the request for the special toroids, our laboratories were not equipped for either.

(Q1) H. P. J. Wijn, Physica 19, 555-564 (1953).

In awaiting the delivery of a 4,000 ampere D.C. supply, we carried out some experiments which resulted in what we consider to be one of the unique discoveries in this work.

For a long time, we have used a cathode-ray oscilloscopic hysteresograph operating at 60 cps. In our arrangement, the field producing winding is a single turn of copper rod 0.4" in diameter, about 3" long. The remainder of the single turn is a copper sheet wound around one leg of the core of a 1 Kva 60 cps transformer. By virtue of the transformation ratio, it is quite feasible to produce peak currents in excess of 5,000 amperes with reasonable line currents.

This arrangement was fixed so that the copper rod was vertical. A cork, bored to fit the rod, was positioned on the rod. A short length of glass tubing was pushed down on the cork so that an annular space was left between the rod and the glass tubing, sealed at the bottom by the cork. Into this annular space was poured a small amount of a slurry of a fine powder of $\text{SrO} \cdot 4 \text{Fe}_2\text{O}_3$. Portions of this powder had previously been used to make permanent magnet samples by the process described in the accompanying Final Report.

It has been a generally accepted view that powders of this nature, when subjected to an a.c. field, would be in a chaotic "dancing" state due to the field reversals. It was with some surprise, therefore, that we observed that, upon the application of the 60 cps field, the powder was immediately drawn to the central conductor (the region of the highest field strength) and remained firmly attached to the rod as long as the current was flowing. A small single crystal

of this material held near to the rod was drawn to the rod and aligned itself with its hexagonal axis in the circumferential direction.

In view of these results, a rough die was constructed and some toroids were pressed in it, orienting the powder with the 60 cps alternating field. The results were encouraging and a die was made for the dimensions of the smaller of the two toroid sizes required.

The 18 toroids of the smaller size (I.D. 0.2") were delivered to the USASNDL on January 24, 1961.

Following this, a die was constructed to press the larger toroids (I.D. 0.5"). Again, the center arbor served as the conductor for the 60 cps current which generated the alternating orienting field in the annular space of the die.

The higher current requirements were met by connecting two of the 1 Kva transformers into the circuit. The primaries of these transformers were connected for single phase 220 V 60 cps, so that, again, high secondary currents could be developed with reasonable line currents. With a line current of 25 amperes RMS, the current through the center arbor was about 11,000 amperes, peak.

One of the troublesome problems in fabricating circumferentially oriented toroids of these materials is that the dimensional shrinkage upon firing is anisotropic (see attached Final Report, "Preparation of Anisotropic Samples"). Upon sintering, the dimension in the direction of the orienting field shrinks more than the two dimensions perpendicular to the field direction. The result of this difference in shrinkage is that, in circumferentially oriented toroids, the

outside and inside circumferences have different shrinkages. Well oriented toroids fired to a high density show a decided tendency to crack radially. This cracking tendency can be alleviated by an increase in the forming pressure and by firing to a somewhat lower density than the maximum sintered density.

The 10 toroids of the larger size (I.D. 0.5") were delivered to the USAFNDL on June 7, 1961.

(b) Demonstration of the Oriented Character of the Toroids

A number of characteristics of sintered oriented materials of this kind are indicative of the fact that the materials are anisotropic. Some of these are:

1. X-ray diffraction patterns taken in (a) the oriented direction and (b) perpendicular to this direction.
2. Magnetic properties in (a) the oriented direction and (b) perpendicular to this direction.
3. If crystallites large enough for visual observation are grown in the sample, then the hexagonal faces of the basal plane are visible on the surface perpendicular to the orienting field whereas only the basal plane edges are visible on the other two surfaces.
4. The anisotropic dimensional shrinkage.

With the cooperation of the X-ray section, we have tried to demonstrate the oriented character of the toroids which were made. This method is a strong method when (1) the samples are large

enough to intercept the full beam of the X-rays in the goniometer and (2) the geometry of the sample is propitious. Neither condition is fulfilled in the case of the toroids made here. This is especially true of the geometry. The pattern obtained from reflections off the basal plane is the most indicative pattern. This requires that the toroid be cut accurately on a radius. We made two such cuts on an oriented toroid. The pattern from one cut showed a ratio of the intensities of the (002) line (which should be enhanced) to the (107) line of 1:4; in the second the ratio was 1:1. Also, because of the small area of the sample, the background was high.

As regards the magnetic properties, the magnetic measurement of these toroids presents a real problem because of the small cross-sectional areas and the relatively high fields required. Measurement in the preferred direction, however, was accomplished with fair accuracy by using the 60 cps hysteresographic technique mentioned above. A photograph of the M versus H trace was taken and the intrinsic induction, $4\pi M$ was manually plotted against H from the photograph and the necessary dimensional information. The peak field strength in the measurement was 3500 oer, the maximum value of $4\pi M$ was 3800 gauss, and the remanence 3300 gauss. This gives a value of the ratio of the remanence to the peak intrinsic induction of 0.87. This result indicates a high degree of orientation.

Our experience has been that the titanium-cobalt substituted materials cannot be induced to grow large crystallites upon sintering. However, $\text{SrO} \cdot 6\text{Fe}_2\text{O}_3$ will grow crystallites which easily reach a

millimeter or more across when viewed on the basal plane (i.e., along the hexagonal axis). We prepared several oriented toroids of $\text{SrO} \cdot 6\text{Fe}_2\text{O}_3$ and obtained crystal growth. These toroids are easily broken and they usually break radially. These radial surfaces give a convincing demonstration of the oriented character of the toroids for they show numerous hexagonal plates of $\text{SrO} \cdot 6\text{Fe}_2\text{O}_3$. In addition, the end surfaces of the toroids show the radial distribution of the edges of the crystallites.

Such a demonstration piece of $\text{SrO} \cdot 6\text{Fe}_2\text{O}_3$ was supplied to the USASRDL with the oriented toroids of $\text{BaO} \cdot 0.48(\text{TiCo})\text{O}_3 \cdot 5.52 \text{Fe}_2\text{O}_3$.

The oriented character of the toroids was also demonstrated by preparing unoriented toroids of $\text{BaO} \cdot 0.48(\text{TiCo})\text{O}_3 \cdot 5.52 \text{Fe}_2\text{O}_3$ and firing them along with oriented toroids of the same material. The O.D. of an unoriented toroid was 1.76 cm whereas that of an oriented sample was 1.52 cm.

Microwave Properties

Ferrimagnetic Resonance in $\text{BaO} \cdot 0.78[(\text{TiCo})\text{O}_3] \cdot 5.22\text{Fe}_2\text{O}_3$

An oriented polycrystalline block of this composition (designated BaTiFe 7a7C1) was received for microwave investigation and an H-plane slab 0.005" thick x 0.050" wide x 2.0" long was fabricated in the usual manner. This was centrally glued to the removable broad wall of a special section of K-band waveguide, similar to the one previously described and constructed for the M band (see Fig. 2 of the Second Quarterly Progress Report for Contract No. DA-

36-039 SC-73223). Ferromagnetic resonance was observed at various frequencies between 20.8 and 25.7 kmc/s in this K band. All resonance lines showed considerable demagnetization losses at low applied fields, as would be expected from the unfavorable geometry and low coercive forces (20 oersteds). As a consequence, the lines were distorted and the linewidths falsified. The same samples were then transferred to the next higher waveguide band (V or U band) and resonance was observed at frequencies between 29 and 32 kmc/s. Low field losses were still present (although barely detectable) at the lower frequencies, while at 32 kmc/s, they were essentially gone. This result is in reasonable agreement with low field loss expectations for a demagnetized ferrite whose anisotropy is of the order of 7000 oersteds, and hence whose maximum frequency for zero field losses ^{Q2,3)} is given by $\gamma(H_{an} + 4\pi M) \sim 25 \text{ kmc/s}$.

From the linear plot of the applied field at resonance against frequency, a value of 2.5 Mc/Oe was obtained for $\gamma/2\pi$. This value seemed somewhat low, and a remeasurement of this quantity on a new H-plane slab gave a value of 2.70, which is the more usual value found in the past for these materials. Since the above-mentioned lower frequency measurements of the resonance lines showed considerable demagnetization, it is believed that their resonance values of H_{ap} were falsified by distortion of the resonance line. Using the resonance

Q2) G. Rado, Rev. Mod. Phys. 25, no. 1, 81 (1953).

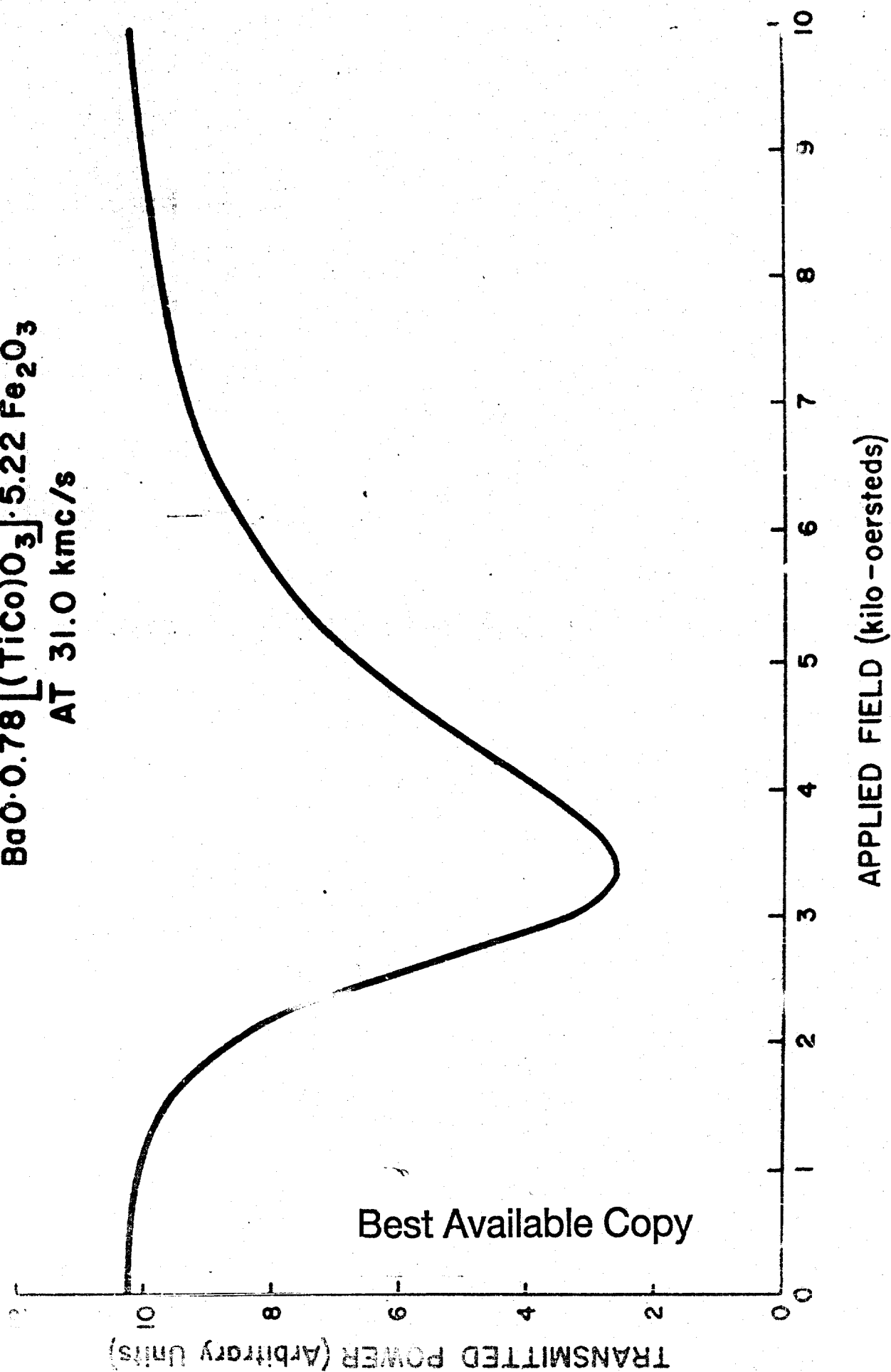
Q3) Ferrites, by J. Smit and H. Wijn, p. 84, Wiley (1959).

data at the highest frequency used (and consequently large values of applied field H_{ap} , which hence showed no distortion) and the value of 2.67 for $\gamma/2\pi$, and the value of 4230 gauss for $4\pi M$ as previously experimentally determined (see Table IV and Fig. 12 of the adjoining Final Report), the value $H_{an} = 6,600$ oersteds was obtained by means of Kittel's relation. Data taken on the new H-plane slab also at large values of H_{ap}^{res} ($H_{ap}^{res} \geq 8000$) gave essentially the same result for H_{an} .

An E-plane slab 0.003" thick x 0.100" high x 0.3" long was investigated next. A typical resonance absorption line obtained with this slab at 31 kmc/s is shown in Fig. Q-1, where the linewidth is seen to be about 2000 oersteds. Resonance lines were also observed at other frequencies between 25 and 40 kmc/s, from which the resulting linear plot of frequency against H_{ap}^{res} gave a value of $\gamma/2\pi = 2.67$, in agreement with past experiments. Using this value and any one of the data points obtained, and assuming $4\pi M = 4230$ gauss as above,* a value of $H_{an} = 6,600$ is obtained by means of Kittel's relation. This value is in close agreement with that obtained for the H plane case; the average value $H_{an} = 6,550$ is then taken as our best determination for this, $x = 0.72$, composition. To compare this value with the theory,

*Actually, an independent value need not have been assumed for $4\pi M$, since the data corresponding to the two above geometries can be solved simultaneously for both $4\pi M$ and H_{an} , using an expanded form of Kittel's formula. The results of such a calculation, using the above-mentioned data, yields $H_{an} = 6400$ and $4\pi M = 4000$ gauss. The reasonable agreement with the results quoted above indicates that this procedure is capable of giving fairly accurate values for both quantities.

Fig. Q-1 TYPICAL RESONANCE ABSORPTION LINE OF AN E-PLANE
 SLAB (0.003" X 0.100" X 0.80") OF
 $\text{BaO} \cdot 0.78 [(\text{TiCo})\text{O}_3] \cdot 5.22 \text{Fe}_2\text{O}_3$
 AT 31.0 kmc/s



i.e., Eq. (8) in the adjoining Final Progress Report, we calculate H_{an} for the composition $x = 0.78$ and find it to be 7,250. Hence the present experimental result appears somewhat lower than anticipated by this theory (see Fig. 13 of the Final Report).

DISTRIBUTION LIST

Report No. 6
Contract No. DA 36-039 SC-85279
Final and Sixth Quarterly Progress Reports

No. of Copies

3	Dr. E. Both Electronic Components Research Department Materials Branch U. S. Army Signal Research and Development Lab. Fort Monmouth, New Jersey
1	Technical Library OASD (R&E) Rm 3E1065 The Pentagon Washington 25, D. C.
1	Commanding Officer U. S. Army Signal Research and Development Agency Fort Monmouth, N. J. ATTN: SIGRA/SL-RE
1	Commanding Officer U. S. Army Signal Research and Development Agency Fort Monmouth, N. J. ATTN: SIGRA/SL-ADT
1	Commanding Officer U. S. Army Signal Research and Development Agency Fort Monmouth, N. J. ATTN: SIGRA/SL-ADJ (MF&R Unit No. 1, ECR Dept.)
3	Commanding Officer U. S. Army Signal Research and Development Agency Fort Monmouth, N. J. ATTN: SIGRA/SL-TN (FOR RETRANSMITTAL TO ACCREDITED BRITISH AND CANADIAN GOVERNMENT REPRESENTATIVES)
3	Commanding Officer U. S. Army Signal Research and Development Agency Fort Monmouth, N. J. ATTN: SIGRA/SL-LNF
1	Commanding Officer U. S. Army Signal Equipment Support Agency Fort Monmouth, N. J. ATTN: SIGMS/ADJ

Best Available Copy

No. of Copies

1
Commanding Officer , ,
U. S. Army Signal Equipment Support Agency
Fort Monmouth, N. J.
ATTN: SIGMS/SDM

1
Director
U. S. Naval Research Laboratory
Washington 25, D. C.
ATTN: Code 2027

1
Commanding Officer and Director
U. S. Navy Electronics Laboratory
San Diego 52, California

2
U. S. Army Signal Liaison Office, WWOL-
Wright Air Development Division
Building 50, Room 025
Wright Patterson Air Force Base, Ohio

1
Commander
Air Force Command and Control Development Div.
Air Research and Development Command
United States Air Force
L. G. Hanscom Field
Bedford, Massachusetts
ATTN: CROTLR-2

1
Commander
Rome Air Development Center
Air Research and Development Command
Griffiss Air Force Base, New York
ATTN: RCSSLD

10
Commander
Armed Services Technical Information Agency
Arlington Hall Station
Arlington 12, Virginia

Advisory Group on Electron Devices
346 Broadway
New York 13, N. Y.

1
Commanding General
Army Ordnance Missile Command Signal Office
Redstone Arsenal, Alabama

Chief, Bureau of Ships
Dept. of the Navy
Washington 25, D. C.
ATTN: 691B2C

Best Available Copy

No. of Copies

1	Commander New York Naval Shipyard Materials Laboratory Brooklyn, New York ATTN: Code 910-d
1	Commanding Officer Diamond Ordnance Fuze Laboratories Washington 25, D. C. ATTN: Technical Reference Section, ORDTL-06.33
1	Commanding Officer Engineering R&D Laboratories Fort Belvoir, Virginia ATTN: Technical Documents Center
2	Chief, U. S. Army Security Agency Arlington Hall Station Arlington 12, Virginia
1	Deputy President U. S. Army Security Agency Board Arlington Hall Station Arlington 12, Virginia
1	Chief, BuOrdinance Navy Department Washington 25, D. C.
1	Ordnance Corps Frankford Arsenal Philadelphia 37, Pennsylvania ATTN: Library, Reports Section
1	Commander Naval Ordnance Laboratory White Oak, Silver Spring 19, Maryland ATTN: Library, Room No. 1-333
1	Chief, Bureau of Aeronautics Department of the Navy Washington 25, D. C.
1	Commanding Officer Watertown Arsenal Watertown, Massachusetts ATTN: OMRO
1	Commanding Officer, 9560 TSU SigC Electronics Research Unit P. O. Box 205 Mountain View, California

Best Available Copy

No. of Copies

1	Commanding Officer USN Underwater Sound Laboratory New London, Connecticut
1	MIT, Lincoln Laboratory Division 6, Group 63 Lexington, Massachusetts ATTN: Librarian
1	Task Order No. EDG6 Engineering Research Institute University of Michigan Ann Arbor, Michigan ATTN: Mr. D. M. Grimes
1	General Electric Corporation Electronics Park Syracuse, New York ATTN: Dr. H. Rothenberg
1	MIT, Lincoln Laboratory Group 84 Lexington, Massachusetts ATTN: Dr. G. S. Heller
1	Harvard University Cruft Laboratory Cambridge, Massachusetts ATTN: Prof. R. V. Jones
1	Research Division Library Raytheon Company 28 Seyon Street Waltham 54, Massachusetts ATTN: Carolyn Joddard
1	Melabs 3300 Hillview Ave. Standard Industrial Park Palo Alto, California ATTN: R. Henscnke
1	Raytheon Company Research Division Waltham 54, Massachusetts ATTN: Dr. Ernst Schloemann
1	R.C.A. David Sarnoff Research Center Princeton, New Jersey ATTN: R. L. Harvey

Best Available Copy

No. of Copies

1
Stanford University
W. W. Hanson Laboratories of Physics
Stanford, California
ATTN: Dr. B. A. Auld

1
Commanding Officer
U. S. Army Signal Research and Development Agency
Fort Monmouth, N. J.
ATTN: SIGRA/SL-PX

1
Commanding Officer
U. S. Army Signal Research and Development Agency
Fort Monmouth, N. J.
ATTN: SIGRA/SL-XE (A. Tauber)

1
Commanding Officer
U. S. Army Signal Research and Development Agency
Fort Monmouth, N. J.
ATTN: SIGRA/SL-PRM (J. Carter)

6
Commanding Officer
U. S. Army Signal Research and Development Agency
Fort Monmouth, N. J.
ATTN: SIGRA/SL-PEM (I. Bady)

1
Marine Corps Liaison Officer
U. S. Army Signal Research and Development Lab.
Fort Monmouth, N. J.
ATTN: SIGRA/SL-LNR

8
N.V. Philips' Gloeilampenfabrieken
Eindhoven, Netherlands
and its affiliates, via:
Department of the Navy
Office of Naval Research
London, England

North American Philips Company, Inc.
Licensing Division
100 East 42nd Street
New York 17, New York
ATTN: Mr. James E. Watkins
(For Licensee Distribution)

Philips Laboratories
A Div. of North American Philips Company, Inc.
Irvington on Hudson, New York
(Internal Distribution)

File

Best Available Copy